

## Technical Report Documentation Page

1. Report No.	2. Government Accession No.	3. Recipient's Catalog No.	
4. Title and Subtitle		5. Report Date	
		6. Performing Organization Code	
7. Author(s)		8. Performing Organization Report No.	
9. Performing Organization Name and Address		10. Work Unit No. (TRAIS)	
		11. Contract or Grant No.	
12. Sponsoring Agency Name and Address		13. Type of Report and Period Covered	
		14. Sponsoring Agency Code	
15. Supplementary Notes			
16. Abstract			
17. Key Words		18. Distribution Statement	
19. Security Classif. (of this report) <b>Unclassified</b>	20. Security Classif. (of this page) <b>Unclassified</b>	21. No. of Pages	22. Price

# JGR Atmospheres

## RESEARCH ARTICLE

10.1029/2021JD034971

### Key Points:

- Stratospheric ozone response of supersonic aircraft emissions depends on altitudes and the sensitivity was found to increase with altitudes
- The ozone impact is small for cruise altitudes below 17 km and the depletion increases sharply as the cruise altitudes increase above 17 km
- Low nitrogen oxides (NOx) combustors may be important to consider for potential future supersonic aircraft with cruise altitudes above 17 km

### Supporting Information:

Supporting Information may be found in the online version of this article.

### Correspondence to:

J. Zhang,  
[jzhan166@illinois.edu](mailto:jzhan166@illinois.edu)

### Citation:

Zhang, J., Wuebbles, D., Kinnison, D., & Baughcum, S. L. (2021). Stratospheric ozone and climate forcing sensitivity to cruise altitudes for fleets of potential supersonic transport aircraft. *Journal of Geophysical Research: Atmospheres*, 126, e2021JD034971. <https://doi.org/10.1029/2021JD034971>

Received 25 MAR 2021

Accepted 31 JUL 2021

© 2021. The Authors.

This is an open access article under the terms of the [Creative Commons Attribution-NonCommercial-NoDerivs License](#), which permits use and distribution in any medium, provided the original work is properly cited, the use is non-commercial and no modifications or adaptations are made.

## Stratospheric Ozone and Climate Forcing Sensitivity to Cruise Altitudes for Fleets of Potential Supersonic Transport Aircraft

Jun Zhang<sup>1</sup> , Donald Wuebbles<sup>1</sup> , Douglas Kinnison<sup>2</sup> , and Steven L. Baughcum<sup>3</sup> 

<sup>1</sup>Department of Atmospheric Sciences, University of Illinois, Urbana, IL, USA, <sup>2</sup>National Center for Atmospheric Research, Boulder, CO, USA, <sup>3</sup>Boeing Company, Seattle, WA, USA

**Abstract** The possibility of commercial and business supersonic aircraft that fly in the lower stratosphere is being discussed and specific designs are under consideration. Emissions from supersonic transports have raised crucial environmental concerns regarding ozone and climate. The atmospheric response is sensitive to a range of factors regarding aircraft types, designs, and deployment parameters. This study conducts a series of sensitivity experiments of possible future cruise altitudes to evaluate the potential atmospheric response for a fleet of supersonic aircraft assumed to be fully operational in 2050. Cruise emissions in the sensitivity studies were varied in 2 km bands over the 13–23 km altitude range. We show that the supersonic aircraft can induce both ozone increase and decrease depending on altitude primarily as a result of emissions of nitrogen oxides, and the changes in total column ozone depend on the cruise altitude. The total column ozone change is shown to have a small increase flying from 13 to 17 km, with the ozone impact not very dependent on cruise altitude. As cruise altitude transitions from 17 to 23 km, the ozone impact transitions from production to depletion and the column ozone depletion strongly depends on cruise altitude. We also explore the seasonal ozone loss, changes in ozone, and climate radiative forcing per unit of fuel burn as a function of cruise altitude. The climate impact of water vapor emissions shows a larger effect associated with higher cruise altitude, with more than 1 mW m<sup>-2</sup> Tg<sup>-1</sup> yr for cruise altitudes above 19 km.

**Plain Language Summary** The impact on stratospheric ozone from potential fleets of supersonic aircraft is of interest for evaluation of possible new aircraft designs. To investigate the sensitivity of atmospheric responses of ozone and radiative forcing from supersonic aircraft emission of nitrogen oxides and water vapor at varying altitudes, this study conducts a series of sensitivity studies as a function of cruise altitude using a global atmospheric chemistry model. The effects on total column ozone and radiative forcing show a strong dependence on cruise altitude, especially for flights above 17 km. Impacts on stratospheric ozone can be reduced by either flying at lower cruise altitudes or by the development of low NOx emitting combustors. This study can potentially help facilitate technological development and optimize aircraft operations towards making supersonic travel environmental friendly.

## 1. Introduction

There is renewed interest in the development of supersonic transport commercial and business aircraft due to a rising demand for more intercontinental air travel as a result of population and economic growth and also a desire for shorter flight times. However, emissions of nitrogen oxides (NOx) and water vapor (H<sub>2</sub>O) from the supersonic aircraft can especially have important environmental effects on ozone and climate (Crutzen 1972, 1974; Dameris et al., 1998; Johnston, 1971; Johnston et al., 1989; Kawa et al., 1999; Kinnison et al., 2020; Penner et al., 1999; Zhang et al., 2021). With most of the emissions taking place in the stratosphere where over 90% of the ozone in the atmosphere is found, fleets of supersonic transport aircraft could have a strong impact on the stratospheric ozone layer. Stratospheric ozone is important because it protects life on Earth from harmful levels of ultraviolet radiation from the Sun and because it is a greenhouse gas that is important to the Earth's climate. In addition, the emissions of stratospheric H<sub>2</sub>O, another important greenhouse gas, from supersonic aircraft exhaust can potentially have a strong warming impact on the climate (Grewe et al., 2007, 2010; Kawa et al., 1999; Penner et al., 1999).

Several more recent studies have evaluated the potential environmental effects of supersonic exhaust on the atmosphere for different specific aircraft designs (e.g., Pitari et al., 2004; Pitari & Mancini, 2001; Grewe et al., 2007, 2010; Zhang et al., 2021). Like the earlier studies, these studies have demonstrated the importance of supersonic NO<sub>x</sub> and H<sub>2</sub>O emissions in the distribution of stratospheric ozone abundance and on climate. Zhang et al. (2021) revisited the potential ozone and climate impacts from the fleet of supersonic aircraft proposed for the earlier assessments—Kawa et al. (1999) and Penner et al. (1999) using a state-of-art climate-chemistry model to update the understanding of potential supersonic aircraft effects, while examining stratospheric ozone sensitivity to different NO<sub>x</sub> emission levels. Previous studies have also shown that the stratospheric ozone effects from fleets of supersonic commercial aircraft are sensitive to cruise altitude (e.g., Baughcum et al., 2003; Grewe et al., 2007, 2010; Wuebbles, Dutta, Jain & Baughcum, 2003; Wuebbles, Dutta, Patten & Baughcum, 2003). This study reexamines this altitude sensitivity of the global atmosphere while holding the fleet emissions constant.

A cross-over point in the ozone chemical production and destruction induced from supersonic aircraft emissions can be found in the lower stratosphere in some of the earlier modeling studies (e.g., Dameris et al., 1998; Grooß et al., 1998; Zhang et al., 2021), but the altitude where this cross-over point occurs is not consistent in the different modeling studies (Grewe et al., 2007). Four models were used in Grewe et al. (2007) and only two of the models simulated a cross-over point in the lower stratosphere. This difference can be attributed to different representations in chemical and transport processes in these models. Using a current state-of-the-art climate-chemistry model, Zhang et al. (2021) found that the cross-over point occurs at altitudes around 17 km over the Northern Hemisphere (NH) mid-latitudes in the lower stratosphere (see Figure 5a). Ozone destruction can be found above this cross-over point all the way up to the middle and upper stratosphere. Below the cross-over point, the addition of the NO<sub>x</sub> emissions from the fleet of supersonic transport aircraft in the model calculations results in an increase in the globally averaged ozone concentrations. This is primarily related to NO<sub>x</sub> chemistry effects on ozone—potentially catalytic ozone destruction in the stratosphere and catalytic ozone formation in the troposphere (Penner et al., 1999). The cruise altitude for a fleet of supersonic transport aircraft determines where emissions occur and the resulting differences in the regions of ozone chemical destruction or production as the emissions are transported to other altitudes and latitudes in the stratosphere. As a result, depending on the cruise altitude, the supersonic fleet emissions can either largely increase or decrease the local ozone concentrations, and the overall globally averaged total column ozone effect is determined by their relative magnitudes of ozone changes at different altitudes.

Earlier studies of Wuebbles, Dutta, Jain and Baughcum (2003), Wuebbles, Dutta, Patten and Baughcum (2003) and Baughcum et al. (2003), investigated the atmospheric ozone and climate sensitivity to cruise altitudes using a parametric approach. The study by Baughcum et al. (2003) evaluated the stratospheric ozone sensitivity to a range of aircraft cruise altitudes using a zonally averaged two-dimensional (2D) model. The results indicated that the calculated total column ozone change was small for cruise altitudes below 15 km altitude and the total column ozone depletion increased significantly as the flight altitudes higher than 15 km. Using a different 2-D model, similar results were found by Wuebbles, Dutta, Jain and Baughcum (2003), Wuebbles, Dutta, Patten and Baughcum (2003) that pointed out emissions near the tropopause at mid-latitudes result in a slight total column ozone increases from 13 to 15 km. Uncertainties in the transport and accumulation of aircraft emissions from the prior studies were significant, particularly for cruise altitudes in the upper troposphere and lower stratosphere. Later studies from SCENIC (Scenario of aircraft emissions and impact studies on chemistry and climate) and HISAC (Environmentally friendly High Speed Aircraft) projects examined altitude sensitivity by assuming specific aircraft concepts to develop emission scenarios for flying at different cruise altitudes (Grewe et al., 2007, 2010). Two emission scenarios with two cruise altitudes of 43–55 and 54–64 kfts (corresponding to 13–16.7 km and 16.5–19.5 km) were aimed at studying the resulting impacts on ozone and climate from different cruise altitudes. The changes in fuel burn and NO<sub>x</sub> emissions were reflected for the two cruise altitudes for the particular aircraft design. Calculations from four three-dimensional (3D) models were carried out in SCENIC and HISAC studies. Both studies found stronger effects on ozone depletion with higher cruise altitudes, while the resulting model-derived ozone changes differ both in magnitude and in patterns across models.

This study is aimed at updating the understanding of the atmospheric sensitivity to cruise altitude for fleets of supersonic aircraft by applying a parametric sensitivity approach. A metric is chosen for the analysis toward decoupling the parametric study from any one particular airplane concept. The conceptual infrastructure configuration of future supersonic aircraft is still under discussion. If a supersonic fleet becomes technically, economically, and environmentally practical, the actual details will depend on the design, range, speed, cruise efficiency, engine characteristics, and market of such an aircraft. Sensitivity studies can help to understand the atmospheric response to a unit emission, which provides useful information to guide the designs to reduce the potential impact of future supersonic aircraft on the global environment.

In this parametric analysis, the High Speed Civil Transport emission scenario from the earlier NASA and IPCC assessment (Kawa et al., 1999; Penner et al., 1999) is used to provide a representative geographical distribution. This study is intended to show how the stratosphere would likely respond to different emission altitudes. The potential effects from the hypothetical fleets of stratospheric-flying aircraft will be evaluated by conducting a series of sensitivity studies in a projected 2050 background atmosphere. The emission scenario here focuses on the NO<sub>x</sub> and H<sub>2</sub>O emissions from a fleet of possible future supersonic aircraft. A state-of-the-art three-dimensional (3D) climate-chemistry model is used to evaluate the sensitivity of the atmosphere, including the troposphere and stratosphere, to different cruise altitudes from possible fleets of supersonic aircraft.

## 2. Methodology

### 2.1. Emission Scenarios

Emission scenarios for possible future supersonic aircraft types depend upon a number of characteristics, including the kind of market (supersonic business jets, commercial airplane), range, constraints (e.g., only flying supersonically over oceans) as well as airplane engine technology. Supersonic aircraft fleets flying at different cruise speeds result in different altitudes with faster aircraft flying higher and with different fuel consumption, and NO<sub>x</sub> emissions. As future aircraft design and technology are still under development and yet undefined for the building of a specific aircraft, a parametric approach is applied in this sensitivity study to explore the atmospheric response from different cruise altitudes, instead of trying to forecast the emission scenarios which resulted from different airplane designs and cruising altitude. In this sensitivity study, the fleet fuel use, NO<sub>x</sub> emission index, and the geographical distribution of the emissions are all held constant while the emission altitude is varied systematically as a function of cruise altitude and applied at 2 km intervals. This 2 km altitude band is intended to capture the sum of many flights going in both directions and is representative of how a fleet would cruise depending on the airplane weight.

The emission inventories were originated and developed by Boeing as a progression from previous studies (Baughcum et al., 1994; Baughcum & Henderson, 1995, 1998). Using the geographical distribution at cruise altitudes and an assumed fleet fuel use (held constant for all altitudes in the parametric study), the emission scenarios used in this sensitivity study are listed in Table S1. The total fuel consumption by this fleet of supersonic aircraft is assumed to be 47.18 Tg/yr. Emission indices of NO<sub>x</sub> and H<sub>2</sub>O stand for the amount of NO<sub>x</sub> and H<sub>2</sub>O emitted in grams per kilogram fuel burn. NO<sub>x</sub> emissions are given on an NO<sub>2</sub> equivalent mass basis. For the NO<sub>x</sub> emission level, it was assumed that the emissions technology is similar to the current subsonic combustor technology with the EI(NO<sub>x</sub>) = 20 g per kg of fuel burn. Initial introduction of commercial supersonic aircraft is likely to use the proven technology. The H<sub>2</sub>O emission level is proportional to the fuel burn and is assumed to be EI(H<sub>2</sub>O) = 1,237 g H<sub>2</sub>O/kg fuel burn. NO<sub>x</sub> and water vapor emissions are intrinsic with any supersonic concept under consideration. Sulfate emissions have been shown to impact ozone chemistry in the stratosphere but are a property of the fuel used and can be minimized by using the low-sulfur jet fuel. Sulfate emissions by the supersonic aircraft are not considered in this sensitivity study, essentially assuming that zero sulfur jet fuel would be used. Sulfate emissions should be considered if evaluating specific design concepts with a well-defined entry into service dates, but that is beyond the scope of this study.

Figure 1 shows the geographical distribution of fuel use as integrated at the cruise altitude; this applies to the eight emission scenarios examined in this sensitivity study. The cruise emissions are assumed to be uniformly distributed vertically over a 2-km band ranging from 13 to 23 km. This 2 km altitude band is

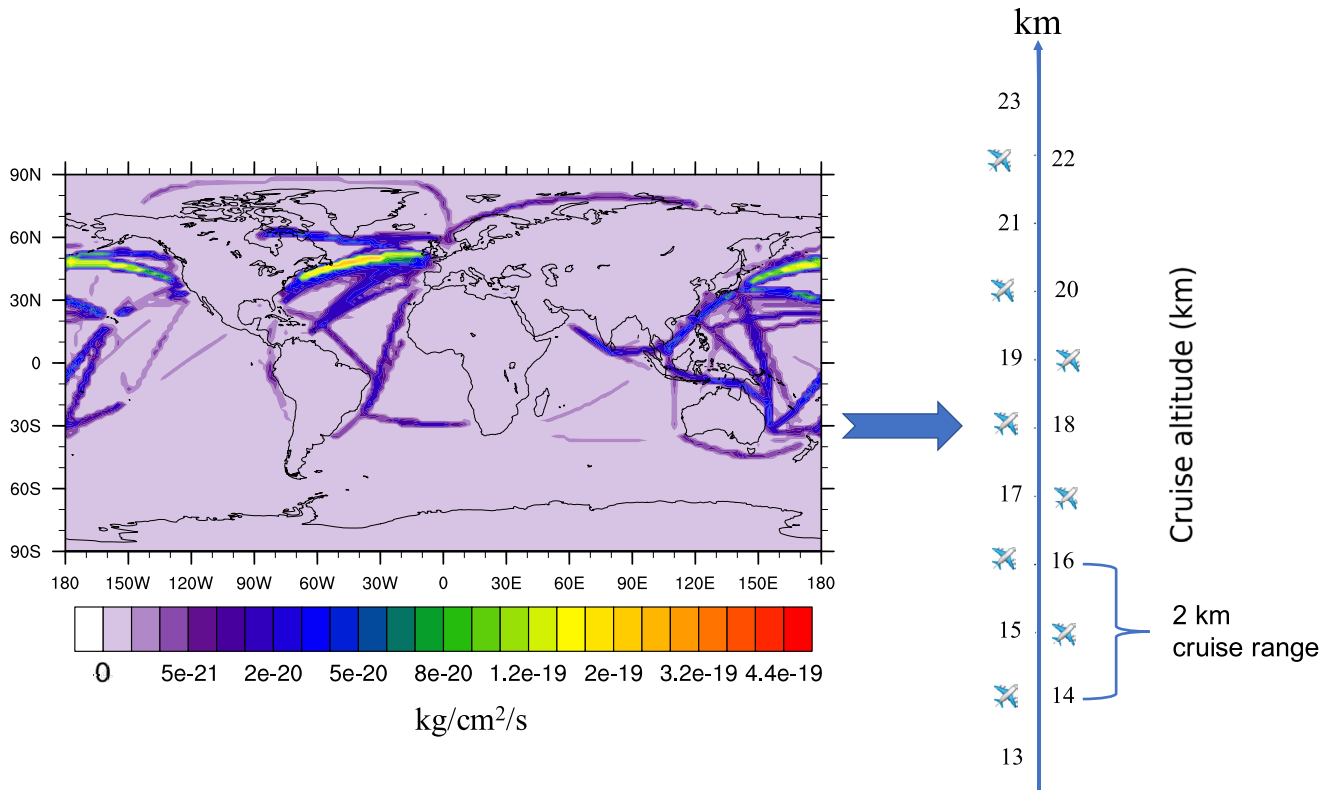


**Figure 1.** Projected distribution of fuel usage ( $\text{kg}/\text{cm}^2/\text{s}$ ) vertically integrated at cruise altitudes for the assumed supersonic aircraft applied to this parametric sensitivity study.

intended to capture the sum of many flights going in both directions and is more representative of how a fleet would operate. Typically, a given airplane type will cruise over a range of 2–3 km of altitude depending on the airplane weight. Aircraft flying in opposing directions along a given flight path are not allowed to fly at the same altitude and so will fly separately in a vertical direction. Fuel burn is especially concentrated to a mid-latitude flight corridor primarily cross the Atlantic and Pacific Oceans, resulting from the market projection of major demand for such an aircraft. The aircraft were assumed to fly supersonically only over water due to concerns about noise from sonic booms in the over-populated regions; as a result, based on market analyses, operations for long-range international transport routes are projected to primarily cross the Atlantic and Pacific Oceans. The majority (~84%) of the fuel burn occurs in the NH, with around 62% of the flights and emissions occurring between 30°N and 60°N.

## 2.2. Model Description and Simulations

The Community Earth System Model/Whole Atmosphere Community Climate Model version 4 (CESM/WACCM4) was used to conduct the numerical experiments. This is a coupled chemistry-climate model from the Earth's surface to the lower thermosphere (Marsh et al., 2013). WACCM is a superset of the Community Atmosphere Model, version 4 (CAM4), and includes all of the physical parameterizations of CAM4 (Neale et al., 2013) and a finite volume dynamical core (Lin, 2004) for tracer advection. WACCM4 used in this study contains a detailed representation of tropospheric and stratospheric chemistry (Kinnison et al., 2007; Lamarque et al., 2012; Tilmes et al., 2016).

The version of WACCM4 model used in this study has been extensively evaluated, including its ability to accurately represent stratospheric ozone (Froidevaux et al., 2019; Garcia et al., 2017; Kunz et al., 2011; Marsh et al., 2013). Froidevaux et al. (2019) has evaluated the stratospheric ozone,  $\text{H}_2\text{O}$ ,  $\text{HCl}$ ,  $\text{N}_2\text{O}$ , and  $\text{HNO}_3$  derived from WACCM4 with observations from the Aura Microwave Limb Sounder (MLS) and Global Ozone Chemistry And Related trace gas Data (GOZCARDS) records for the Stratosphere. This model-data

comparison has focused on the absolute abundances, variability, and trends as well as the longer term series of these species. Results show that climatological averages for 2005–2014 from WACCM compare favorably with observation data averages over this period. The WACCM ozone trends generally agree (within  $2\sigma$  uncertainties) with the MLS data trends. For  $\text{H}_2\text{O}$ , WACCM and MLS both show similar short-term positive trends and the abundances also agree well—within  $\sim 5\%$  and  $\sim 10\%$  difference in the stratosphere and mesosphere respectively. For  $\text{HCl}$ ,  $\text{N}_2\text{O}$ , and  $\text{HNO}_3$ , the short-term trend profiles from MLS are well captured and matched by WACCM trends for these species in the stratosphere.

The middle atmospheric dynamics (e.g., temperature, zonal and meridional winds, and surface pressure) have also been evaluated relative to observations from previous studies (Froidevaux et al., 2019; Garcia et al., 2019; Marsh et al., 2013), as summarized in Zhang et al., 2021. These dynamic factors are driving the physical parameterization controlling boundary layer exchanges, advective and convective transport, and the hydrological cycle. The convection schemes used in the model originated from the studies of Zhang and McFarlane (1995) as well as Bretherton and Park (2009) for deep convection scheme and shallow convection scheme, respectively. These schemes have been widely evaluated and used in CAM4 and CAM5 (Neale et al., 2013; Yang et al., 2013).

The stratospheric-adjusted radiative forcing attributable to the calculated changes in ozone and  $\text{H}_2\text{O}$  is estimated using the Parallel Offline Radiative Transfer (PORT) model (Conley et al., 2013). PORT utilizes the radiation code from CAM4 (Gent et al., 2011) and calculates the changes in the stratospheric-adjusted radiative forcing under the fixed dynamical heating condition (Fels et al., 1980). A more detailed description for WACCM and PORT can be found in Zhang et al., 2021.

Simulations in this study are branched off from the existing Chemistry Climate Model Initiative (CCMI) simulations for the model years 2040–2052 (Morgenstern et al., 2017) and outputting the high frequency meteorological fields, sea surface temperatures, and sea ice for the same time period. All the simulations used in this study are running with the specified dynamics (SD) mode (Lamarque et al., 2012) using the derived information from the CCMI runs. All the model simulations include an identical Quasi Biennial Oscillation (QBO) that is nudged to hindcast of observation, that is, a repeating sequence of existing observations is used for the future period (Matthes et al., 2010). The meteorology fields have been externally nudged to the high frequency meteorological output up through 120 km. The horizontal resolution of the simulation is  $1.9^\circ$  latitude  $\times$   $2.5^\circ$  longitude with 66 vertical levels from the surface up to about 140 km. The vertical resolution in the lower stratosphere ranges from  $\sim 1$  km near the tropopause to about 2 km near the stratopause. The reference run is first performed for a 2050 background atmosphere without the supersonic aircraft emissions. Then the experiment runs are conducted by adding supersonic perturbations on top of the reference run. The emissions from subsonic air traffic are not accounted for to examine changes induced due to a supersonic fleet only. For each of the simulations, the model was driven with the same meteorology fields, kinetic reactions, heating rates, and climatology files, yet only varying with aircraft emission input files according to the scenarios studied. The difference between the perturbed and reference background simulations are the changes induced from the supersonic aircraft emissions, excluding dynamics-chemical feedbacks. For the emission scenarios evaluated in this study, all the results are evaluated once the model has reached a steady state relative to the prescribed background atmosphere. The results from the last three years are taken into analysis due to the slightly different effects on ozone for the different phases of the QBO.

### 3. Model Projection of Source Gases and the Background Atmosphere

The effect of supersonic aircraft emissions depends on the future background atmosphere in which the aircraft will fly. Supersonic emissions would operate in a future stratosphere that will likely have different trace constituent mixing ratios and aerosol abundances than the current atmosphere. Climate change will also change stratospheric temperatures and winds, along with changes in the troposphere and at the tropopause. The increased greenhouse gases are assumed to accelerate the Brewer-Dobson Circulation and result in the decrease of tropic ozone and increase of higher latitude ozone in the stratosphere (Butchart, 2014). The human-related emissions of chlorine- and bromine-containing chemicals after the industrial revolution have had a significant influence on stratospheric ozone. The potential future supersonic aircraft emissions can also affect stratospheric ozone via the  $\text{NO}_x$  and  $\text{HO}_x$  odd-oxygen loss cycles. The future evolution of ozone

will depend on the assumed levels of the various source gases (such as  $\text{N}_2\text{O}$ ,  $\text{CH}_4$ , and  $\text{CO}_2$ ); levels of these greenhouse gases could be affected by the future climate policy and this could significantly influence the estimated ozone perturbation from the assumed supersonic fleet (Butler et al., 2016; Portmann et al., 2012; Ravishankara et al., 2009).

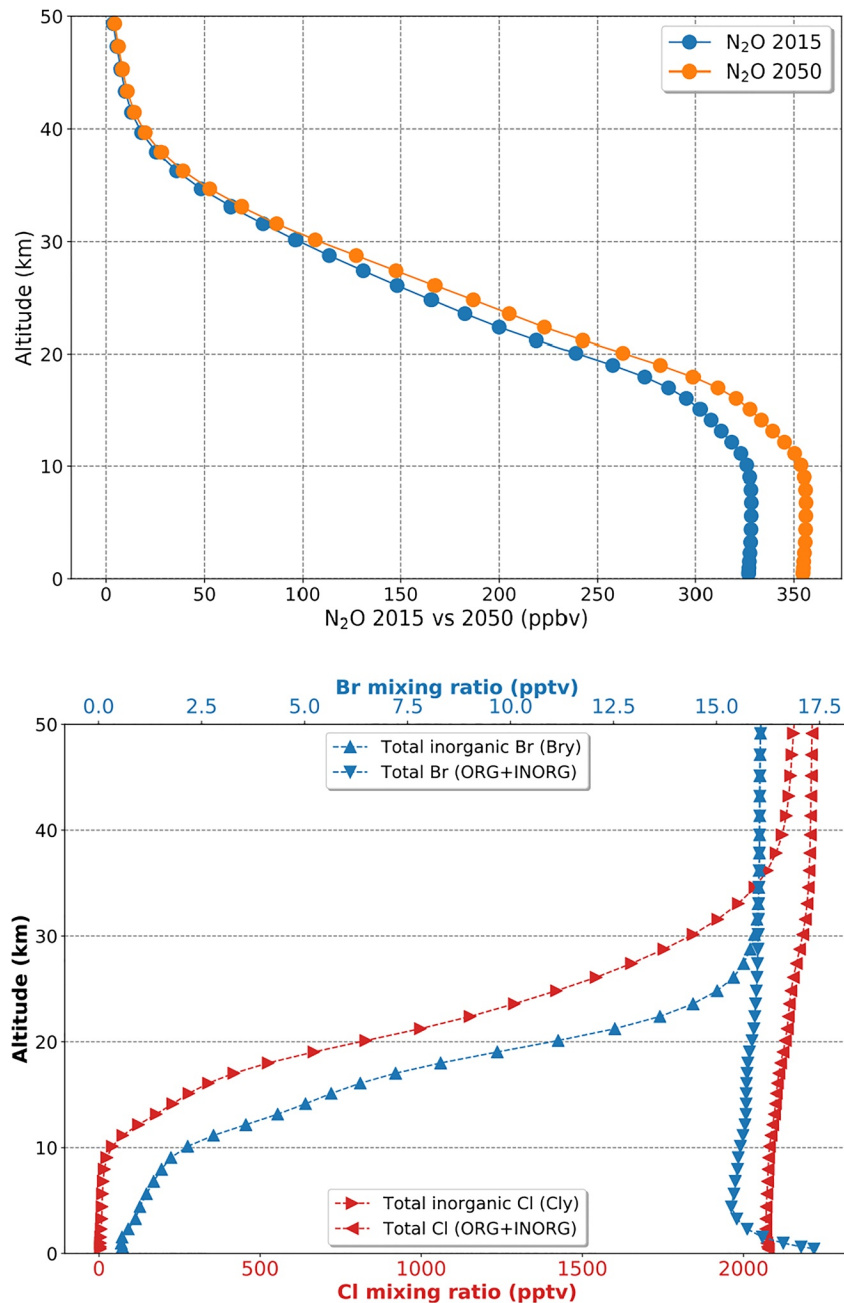
Source gas boundary conditions used in this study for the 2050 background atmospheres are based on the Coupled Model Intercomparison Project Phase 5 with improvements on latitudinal and seasonal gradients (Meinshausen et al., 2011). The projection is following the climate change trajectory of the Representative Concentration Pathways 6.0 (Van Vuuren et al., 2011). The reference background atmosphere assumed in this study includes a sulfate surface area density that is representative of a volcanically clean atmosphere. Projected future species by species source gas in the 2050 boundary conditions at the Earth's surface adopted in this study can be found in Table S2, with the values for 2015 boundary conditions listed here for comparison. WACCM derived background  $\text{N}_2\text{O}$  profiles for the 2050 conditions are shown in Figure 2a, with the model-derived 2015 condition also shown for comparison. The vertical profile of  $\text{N}_2\text{O}$  indicates a sharp decrease starting from the upper troposphere and lower stratosphere all the way up to the stratopause, as  $\text{N}_2\text{O}$  is mostly photolyzed into  $\text{N}_2$ . The  $\text{N}_2\text{O}$  profile shows a higher concentration in the year 2050 compared to the year 2015 in the stratosphere.

Figure 2b shows that the model derived global averaged chlorine and bromine mixing ratio changes as a function of altitude for the projected 2050 conditions. Both the total species of Cl and Br (organic + inorganic), as well as the total inorganic species of Cly and Bry are shown in Figure 1d. The fraction of inorganic Cl and Br both increases with rising altitudes, especially between 13 and 23 km cruise altitude. The model derives a level of 2.1 ppbv total inorganic chlorine Cly (i.e.,  $\text{Cl} + \text{ClO} + 2\text{Cl}_2 + 2\text{Cl}_2\text{O}_2 + \text{OCIO} + \text{HOCl} + \text{ClO-NO}_2 + \text{HCl} + \text{BrCl}$ ) and 16 pptv total inorganic bromine Bry (i.e.,  $\text{Br} + \text{BrO} + \text{HOBr} + \text{BrONO}_2 + \text{HBr} + \text{BrCl}$ ), respectively at the top of the stratosphere. These values have declined to  $\sim 34\%$  and  $\sim 20\%$  compared to the 2015 boundary conditions for the Cly and Bry levels, respectively, due to the legally binding controls on the production of most human-produced halogenated gases known to destroy ozone.

## 4. Results and Discussion

### 4.1. Emissions of Nitrogen Oxides and Water Vapor From Supersonic Transport

Effects on atmospheric composition due to the supersonic aircraft emissions are shown through the change in the zonal and annual mean concentrations of  $\text{NO}_y$  and  $\text{H}_2\text{O}$ .  $\text{NO}_y$  is the total inorganic nitrogen ( $\text{NO}_y = \text{N} + \text{NO} + \text{NO}_2 + \text{NO}_3 + 2\text{N}_2\text{O}_5 + \text{HO}_2\text{NO}_2 + \text{HNO}_3 + \text{ClONO}_2 + \text{BrONO}_2$ ); this includes the most reactive nitrogen oxides, referred to as  $\text{NO}_x$  ( $\text{NO} + \text{NO}_2$ ) and other species such as  $\text{N}_2\text{O}_5$  and  $\text{HNO}_3$ . Figures 3a and 3b show the perturbation in annual-averaged  $\text{NO}_y$  (ppbv) and  $\text{H}_2\text{O}$  (ppmv) concentrations from supersonic aircraft emissions relative to the background atmosphere for cruise altitudes at 21–23 km case. To provide a more illustrative view of the resulting impact, we show the perturbations from the highest cruise altitude in this sensitivity study here and in the following analysis. Other cases are shown in the line plots Figures 3c and 3d in the Northern Hemispheres for comparison. For a range of cruise altitude between 13 and 23 km, distinct enhanced  $\text{NO}_y$  and  $\text{H}_2\text{O}$  concentrations are found at the altitudes where the supersonic emissions occur for all parametric study experiments. The enhancements take place in both hemispheres with a much larger fraction occurring in the NH, as expected. The magnitude of the  $\text{NO}_y$  and  $\text{H}_2\text{O}$  enhancement (in ppbv and ppmv, respectively) in both hemispheres increases with increasing emission altitudes (Figure S1). This increase is because the density of air is exponentially decreasing with altitude, thus the same amount of emission results in a larger mixing ratio with height. The maximum perturbation of 9 ppbv is found over the NH mid-latitudes for the 21–23 km cruise altitude. The difference between the  $\text{NO}_y$  and  $\text{H}_2\text{O}$  perturbations is that a much larger fraction of emitted  $\text{H}_2\text{O}$  is transported southward across the tropics to the SH as well as transported upward to the stratopause into the mesosphere. This is due to the differences in their atmospheric lifetimes, with around 1 year and 3 months lifetime in the upper stratosphere for  $\text{H}_2\text{O}$  and  $\text{NO}_y$ , respectively (Kinnison et al., 2020). At cruise altitudes from 21 to 23 km, the maximum local  $\text{H}_2\text{O}$  concentration increase reaches 1.5 ppmv at NH mid-latitudes and the stratospheric column  $\text{H}_2\text{O}$  increase by 4.45% in the NH average. The perturbation in  $\text{H}_2\text{O}$  has a similar pattern and gradient to that found by Grewe et al. (2007) (see their Figure 3), but with a different magnitude; this difference



**Figure 2.** Whole Atmosphere Community Climate Model (WACCM) derived annual and global average in (a) N<sub>2</sub>O as the function of altitudes in the year 2050 on comparison to 2015; Panel (b): total inorganic chlorine (Cl) and bromine (Br) and the corresponding total Cl and Br (organic + inorganic) in 2050. Cl mixing ratio is shown in red with the lower labels while Br mixing ratio is in blue with the upper labels.

is mainly due to the differences in aircraft designs and emission scenarios (i.e., the fuel consumption from Grewe et al. [2007] is 60 Tg/yr compared to 47.18 Tg/yr in our study).

Emissions primarily occur in the lower stratosphere of the NH, with a relatively small fraction transported to the SH along with the emissions that actually occur in the SH. At lower cruise altitudes (lower than 17 km), the model-derived gradient of the spread in NO<sub>y</sub> and H<sub>2</sub>O is small in the lower stratosphere from NH mid-latitudes to SH high latitudes (Figure S1). Above 17 km, more NO<sub>y</sub> and H<sub>2</sub>O is lifted to the middle and upper stratosphere and also transported to the SH with increasing injection altitude. The spread in NO<sub>y</sub>



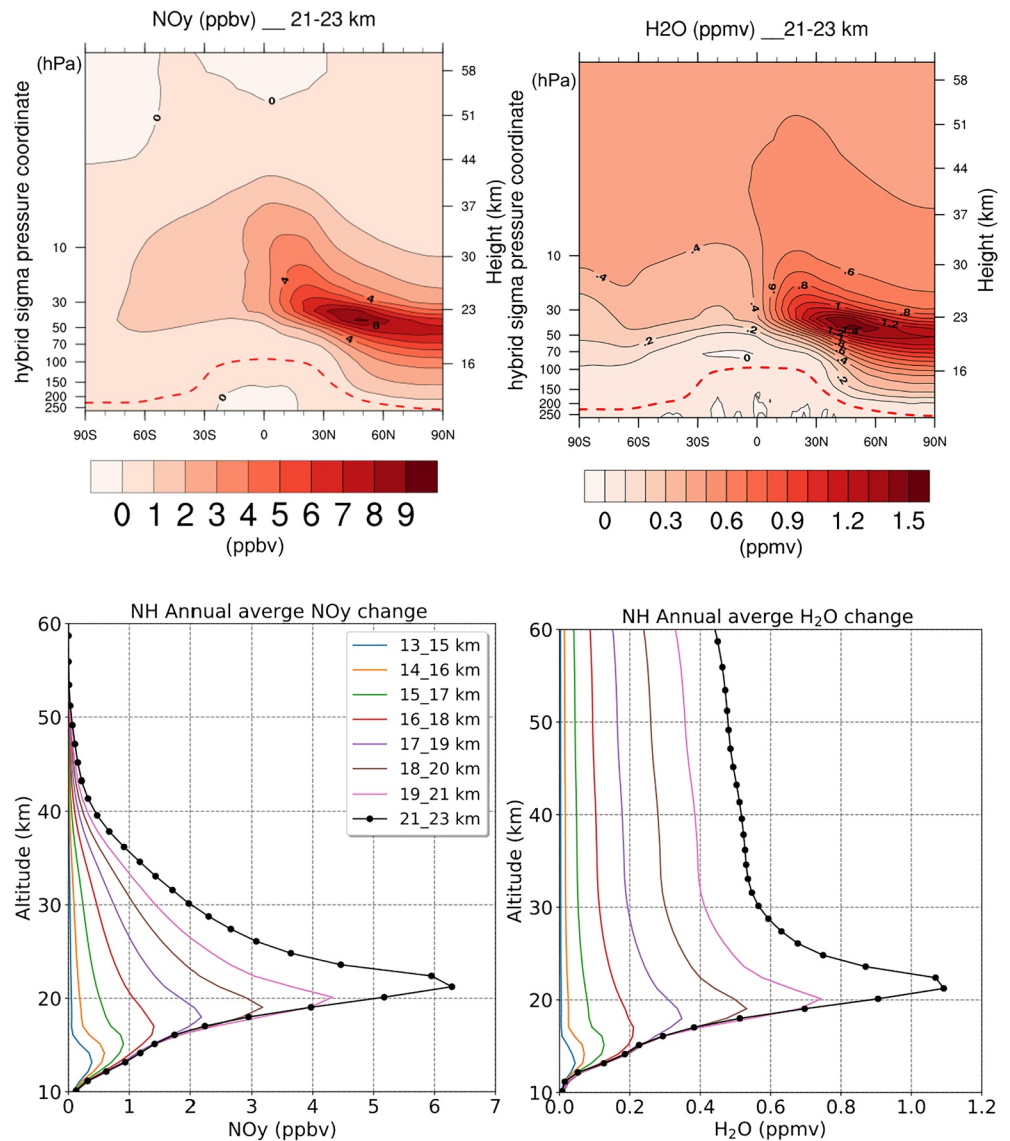


**Figure 3.** Calculated supersonic aircraft emission induced annually averaged change in (a) NO<sub>y</sub> (ppbv) and (b) H<sub>2</sub>O (ppmv) for cruise altitudes at 21–23 km, the red dashed line indicates the location of the lapse rate tropopause; Northern hemispheric annual average change in (c) NO<sub>y</sub> (ppbv) and (d) H<sub>2</sub>O (ppmv) for eight sensitivity cases. The results from Case 21–23 km are shown in black dotted lines.

and H<sub>2</sub>O changes across all the parametric scenarios contributing to differences in the ozone fields for the range of supersonic aircraft-induced perturbations.

#### 4.2. Ozone Response to the Supersonic Transport Emission

The distribution of ozone is determined by a complex balance between transport and chemical production and destruction (Brasseur, 2020; WMO, 2018). Transport processes influence ozone concentration both by transporting ozone itself and also by the transport of precursors that induce ozone chemical production and transport of other gases that lead to the destruction of ozone (e.g., NO<sub>x</sub> and H<sub>2</sub>O emitted from aircraft). The Brewer–Dobson circulation (BDC) is a residual meridional circulation in the stratosphere driven largely by the deposition of momentum by planetary-scale waves. This residual circulation will be the predominant means of transporting emissions to the middle and upper stratosphere within the tropics, while at the middle and high latitudes, this circulation is responsible for transport of exhaust into the lowermost

stratosphere. Changes in the BDC of tropical upwelling have been shown to have a statistically significant impact on ozone in the mid-latitude lower stratosphere (Neu et al., 2014). In addition, the quasi-horizontal mixing can contribute to transport from mid-latitude flight corridors into the tropical region.

It is expected that most of supersonic commercial aircraft emissions assumed in this study would occur in the lower stratosphere at NH mid-latitudes. The effect of the emissions on global ozone levels will depend on how rapidly the exhaust is dispersed into different regions of the stratosphere and to what extent the pollutants can build up and accumulate. The resulting distribution of supersonic aircraft emissions will depend on the local residence time which is correlated with the mean age of air. The mean age of stratospheric air is an estimate of the time of residence of an air parcel in the stratosphere (Hall & Plumb, 1994; Waugh & Hall, 2002) which is mainly dependent on the strengths of, and balance between the residual circulation and quasi-horizontal mixing. Previous independent observations indicate the ages of air to be about 4–6 years in the lower stratosphere mid-latitudes ( $\sim 40\text{--}60^\circ\text{N}$ ,  $\sim 20\text{--}25$  km) (Haenel et al., 2015). At the same latitudes, the annual mean climatology of mean age of air derived from the satellite data shows an increase with increasing height in the stratosphere (WMO, 2018). With increasing cruise altitude in this sensitivity study, the supersonic aircraft emissions will be emitted into a region with an older mean age and associated with a longer residence time. The residence time at different locations can affect the accumulation of aircraft emissions which can further influence the resulting ozone changes in the stratosphere before the emissions get transported to and removed in the troposphere.

The annually averaged percentage changes in ozone are shown in Figure 4 for the range of cruise altitudes. The ozone change is the result of combined effects from emissions of NO<sub>x</sub> and H<sub>2</sub>O from the assumed fleet of supersonic aircraft. For cruise altitudes from 21 to 23 km (Figure 4a), there is an ozone production zone near the upper troposphere and lower stratosphere in both hemispheres. Reduction of ozone is found in the middle to upper stratosphere and into the mesosphere. The maximum ozone depletion in percentage for the 21–23 km case peaks over the NH high latitudes at the emission altitudes with a reduction of  $-14\%$ . The reduction extends southward to the tropics and SH, with a larger fraction of ozone depletion confined in the NH. Compared to the 21–23 km emissions, the cruise altitude at 17–19 km (Figure 4b) shows a larger ozone increase near the tropopause and weaker ozone reduction near the cruise altitudes. The simulated ozone changes from four model results in Grewe et al. (2007) also found an ozone decrease at the higher altitude in the stratosphere (their Figure 4), while only the ULAQ and E39/C models in their study found ozone increase near the tropopause.

Figure 4c depicts the vertical profile of ozone change for the 17–19 km and the 21–23 km emission cases at  $10^\circ\text{N}$  and  $42^\circ\text{N}$ , respectively. At lower latitudes with higher tropopause height, the ozone production region can extend much higher than at higher latitudes—the ozone increase turning into ozone decrease at around 23.5 and 24.5 km for 21–23 km and 17–19 km cases at  $10^\circ\text{N}$ , while the turning point is at around 12 and 17.5 km at  $42^\circ\text{N}$  for 21–23 km and 17–19 km case, respectively. The ozone production and reduction due to the NO<sub>x</sub> and H<sub>2</sub>O emissions from the supersonic aircraft fleet occur in each of the emission scenario, and this reduction is particularly distinct for cases with cruise emissions above 17 km (Figure 4d). The magnitude of ozone depletion increases with the cruise altitude of the supersonic aircraft, with the maximum depletion in percentage occurring near the emission altitude. For higher emissions altitudes, more ozone depletion occurs in the SH, which corresponds to the larger amount of emitted NO<sub>y</sub> and H<sub>2</sub>O transported across the equator and dispersed in the SH (Figure 3).

The ozone increase near the tropopause (Figure 4a) can be attributed to a combination of the direct effects of enhanced ozone production from NO<sub>x</sub> emissions through a combination of different processes: smog-like chemistry, the ozone self-healing effect resulting from the ozone depletion at higher altitudes, and a decrease in the ozone loss rates in this region due to the interference of the emitted NO<sub>x</sub> with the HO<sub>x</sub> ozone loss cycle. Figure 5a shows the background annual mean of ozone production due to the three mechanisms at  $10^\circ\text{N}$  and  $42^\circ\text{N}$ —smog chemistry production, total Odd Ox production, as well as the Ox loss rate due to the NO<sub>x</sub> and HO<sub>x</sub> family cycles. Two latitudes,  $10^\circ\text{N}$  and  $42^\circ\text{N}$ , are shown here to illustrate the mechanisms producing the ozone increases in the extratropics and mid-latitudes, respectively. A 10% contribution of smog production to the overall ozone production can be found in the stratosphere at around 30 km for latitudes  $10^\circ\text{N}$  and  $42^\circ\text{N}$ . At  $42^\circ\text{N}$  mid-latitude, the NO<sub>x</sub>-induced ozone loss surpasses the NO<sub>x</sub>-induced ozone production at around 20 km, while this inflection point is around 22.5 km at  $10^\circ\text{N}$ . Similarly, the height

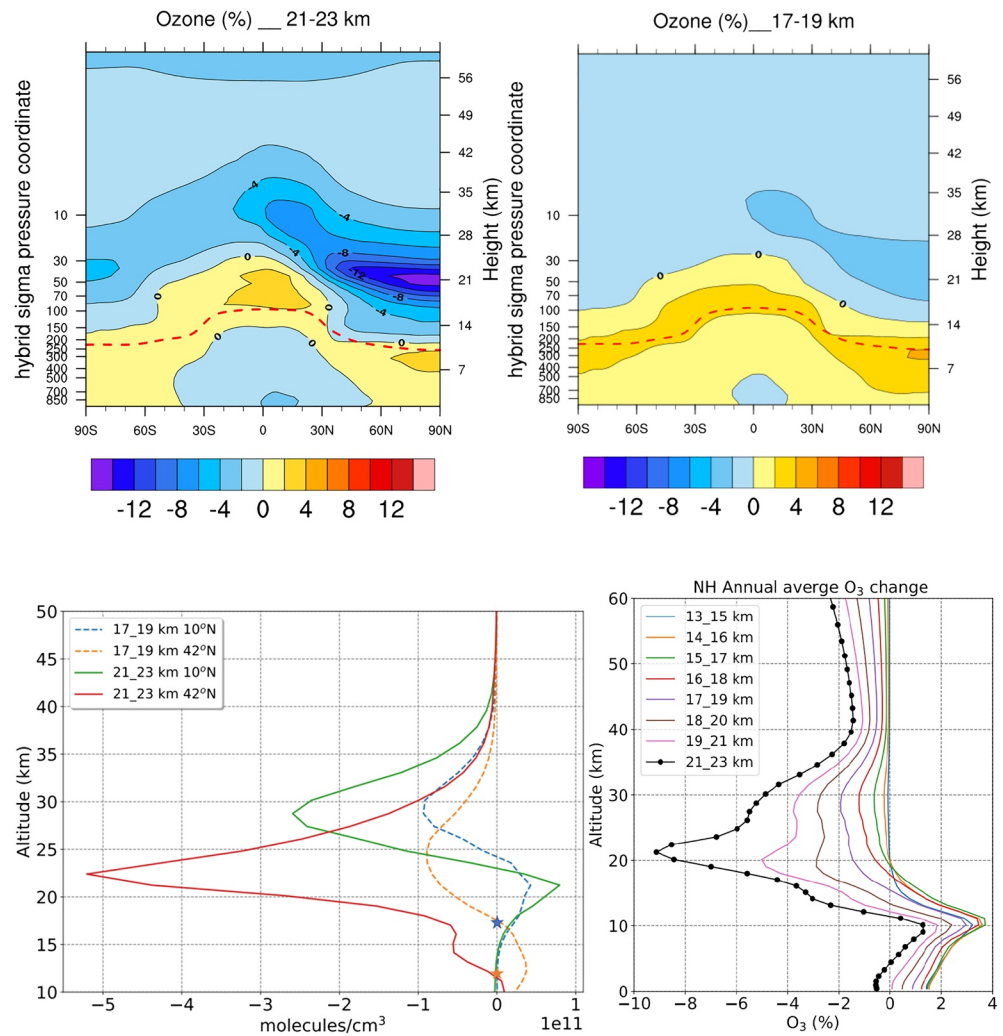


**Figure 4.** Calculated supersonic aircraft emission induced annually averaged change in ozone change (in % change except for [c]) for cruise altitudes at (a) 21–23 km and (b) 17–19 km; (c) Annual average change in ozone (molecule/cm<sup>3</sup>) at 10°N and 42°N for cruise altitudes at 21–23 km and 17–19 km. The blue and orange stars indicate the tropopause height at 10°N and 42°N. (d) Northern hemispheric annual average percentage change in ozone for all sensitivity cases.

where the NO<sub>x</sub> induced ozone loss surpasses HO<sub>x</sub>-induced ozone loss is around 24.5 km at 10°N, higher than the 21.5 km at 42°N. These differences are due to the much larger NO<sub>x</sub>-induced ozone loss at 42°N compared to 10°N. Between 10 and 30 km, the total O<sub>x</sub> production rate is stronger at 10°N than mid-latitude 42°N at the same altitude, owing to stronger exposure to solar ultraviolet light at lower latitudes.

Figures 5b and 5c show the supersonic aircraft emission-induced changes (perturbation—reference) at 42°N and 10°N, respectively. The ozone production at the upper troposphere and lower stratosphere (tropopause around 12 km) for 42°N is mainly attributed to the NO<sub>x</sub> emissions enhancing the NO<sub>x</sub>-ozone production through smog chemistry. In addition, a decrease in the ozone loss rates in this region due to the interference of the emitted NO<sub>x</sub> with the HO<sub>x</sub> ozone loss cycle also contributes to this ozone increase. Self-healing effect plays minimal role on the ozone increase at 42°N. The situation is quite different at 10°N lower latitude, where the ozone increase near the tropopause (around 17.5 km) is mainly due to the self-healing effect. At both latitudes, NO<sub>x</sub> induced ozone loss is largely dominant over HO<sub>x</sub>-induced ozone loss for altitudes from the lower to middle stratosphere, which is consistent with previous supersonic aircraft studies (e.g., Grewe et al., 2007; Wuebbles, Dutta, Jain & Baughcum, 2003; Wuebbles, Dutta, Patten & Baughcum, 2003).

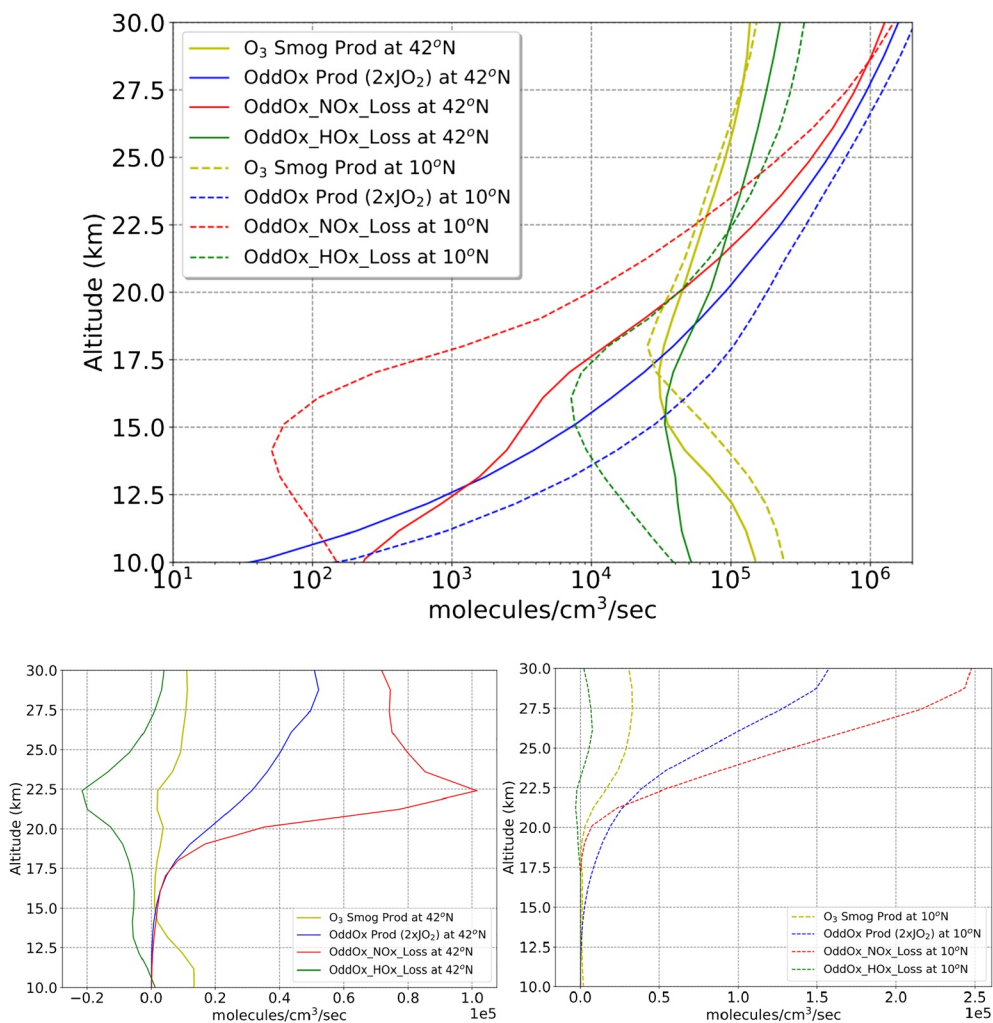


**Figure 5.** (a) Background annual mean of ozone production due to smog chemistry (yellow line)  $O_3\_Smog\_Prod = NO\_HO_2 + CH_3O_2\_NO + \text{multiple NHMC\_NO}$ , total Ox product (blue line)  $2^*JO_2 = O_2 + hv \Rightarrow 2O$ , NO<sub>x</sub>-induced ozone loss (red line) defined in Text S1, HO<sub>x</sub>-induced ozone loss (green line) defined in Text S1. Solid lines are at 42°N and dashed lines are for 10°N; (b) and (c) are the supersonic aircraft emission-induced changes (perturbation run—reference run) at 42°N and 10°N, respectively. Positive values for total Ox product (OddOx Prod) indicate the self-healing effect. The above figures are shown for cruise altitude at 21–23 km.

Figure 6 shows the odd oxygen (Ox = O + O<sub>3</sub>) chemical loss mechanisms for the NH average for the NO<sub>x</sub>, HO<sub>x</sub>, and halogen oxide catalytic cycles (ClO<sub>x</sub> and BrO<sub>x</sub>, which are combined here to show interactions relative to the NO<sub>x</sub> and HO<sub>x</sub> cycles), as well as by the Chapman Ox self-destruction loss reactions (Crutzen & Ehhalt, 1977; Portmann et al., 2012). The definition of Ox and the reactions included in each catalytic cycle are based on the definitions in Brasseur and Solomon (2005). The background Ox loss in the NH from all four loss cycles and the resulting total loss are shown in Figure 6a, which indicates that the NO<sub>x</sub> involved the Ox loss cycle (NO<sub>x</sub>-Ox) and HO<sub>x</sub> involved the Ox loss cycle (HO<sub>x</sub>-Ox); both play important roles on the total Ox loss yet at different altitudes. The NO<sub>x</sub>-Ox cycle is the primary loss mechanism between 30 and 40 km and the maximum effect of the HO<sub>x</sub>-Ox loss cycle is above 40 km. The loss from the Ox self-loss cycle (Ox-Ox) and ClO<sub>x</sub>/BrO<sub>x</sub> involved the Ox loss cycle (ClO<sub>x</sub>/BrO<sub>x</sub>-Ox) are important from 30 to 50 km, but overall to a much less degree compared to the NO<sub>x</sub>-Ox and HO<sub>x</sub>-Ox cycles on the NH average. At the upper troposphere and lower stratosphere, the HO<sub>x</sub>-Ox cycle is the dominant Ox loss, and the NO<sub>x</sub>-Ox loss surpasses the HO<sub>x</sub>-Ox loss at 20 km. Compared to the background total Ox loss to the 2015 conditions (Figure 6a in Zhang et al., 2021), the total Ox loss in 2050 has reduced which is predominately due to the reduction of Ox loss from ClO<sub>x</sub> and BrO<sub>x</sub> catalytic cycles.

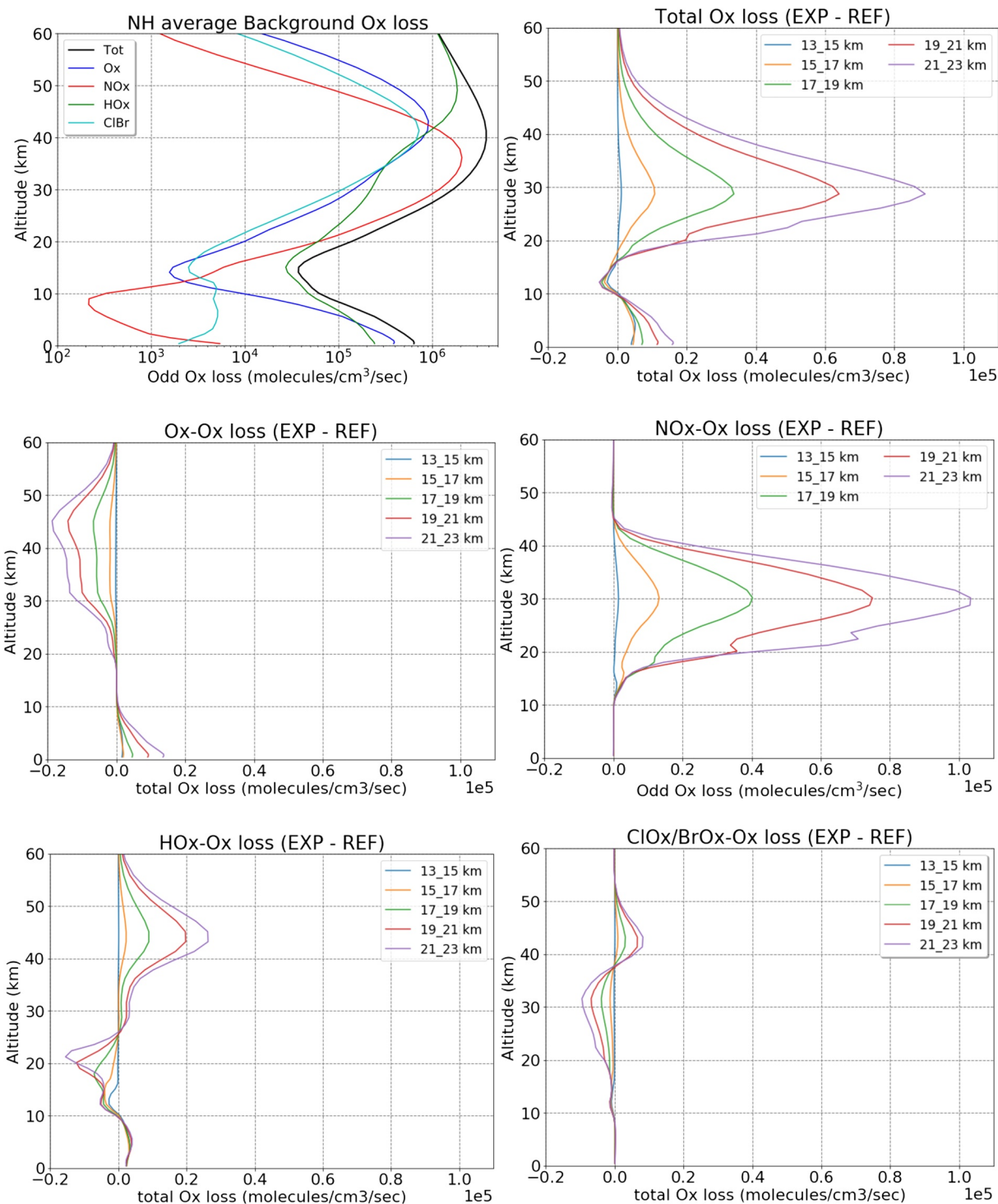


**Figure 6.** Annually and Northern Hemisphere (NH)-averaged profile of odd oxygen (Ox) chemical loss rates by catalytic cycles involving NOx, HOx, and halogens as well as the chemical loss by the Chapman mechanism (Ox) for: Panel (a) background condition without supersonic aircraft emissions; Panel (b): total odd Ox loss due to all loss mechanisms (perturbations - background) for each emission scenario; Changes of (c) Ox-Ox loss; (d) NOx-Ox loss; (e) HOx-Ox loss; (f) ClOx/BrOx-Ox loss, respectively. Different color lines represent different cruise altitudes, with only every other sensitivity study plotted for better readability. All lines are valid between 0 and 60 km. The definition of these chemical cycles can be found in Text S1.

Emissions from supersonic aircraft result in perturbations of the catalytic ozone destruction cycles involving NO<sub>x</sub>, HO<sub>x</sub>, ClO<sub>x</sub>, and BrO<sub>x</sub> species by causing a repartitioning between the chemical families. The NH averaged supersonic aircraft induced changes in total Ox loss, Ox-Ox loss, NO<sub>x</sub>-Ox loss, HO<sub>x</sub>-Ox loss, and ClO<sub>x</sub>/BrO<sub>x</sub>-Ox loss for all sensitivity cases are shown in Figures 6b–6f, respectively. These delta changes are calculated from the perturbed emission scenarios relative to the background atmosphere and then averaged over the NH. The color lines in each figure represent cases with emission at different cruise altitudes. The vertical profile of total Ox loss (Figure 6b) shows that the maximum loss occurs at around 30 km for all cases, which is largely attributed to the NO<sub>x</sub>-Ox loss cycle. The contribution of HO<sub>x</sub>-Ox loss to the total Ox loss is mainly in the upper stratosphere from 40 to 50 km, while this effect is largely cancelled out by the reduction of Ox-Ox loss. With the additional H<sub>2</sub>O perturbation from supersonic aircraft emission, more Ox is destroyed by the HO<sub>x</sub>-Ox loss cycle, which results in the reduction of Ox-Ox loss at the same location. The halogen involved Ox loss decreases at around 30 km, which is due to the supersonic transport-induced NO<sub>x</sub> and HO<sub>x</sub> interfering with the halogen cycles by taking some of the reactive chlorine and bromine and converting them into the relatively less reactive reservoirs (e.g., ClONO<sub>2</sub>). The enhanced ClO<sub>x</sub>/BrO<sub>x</sub>-Ox loss above 40 km is due to more ClO production from the coupling reaction with HO<sub>x</sub>, which then triggers more ozone loss due to the Cl cycle. All the emission scenarios share a similar vertical profile of each Ox loss cycle, while a stronger effect is associated with a higher emission altitude.

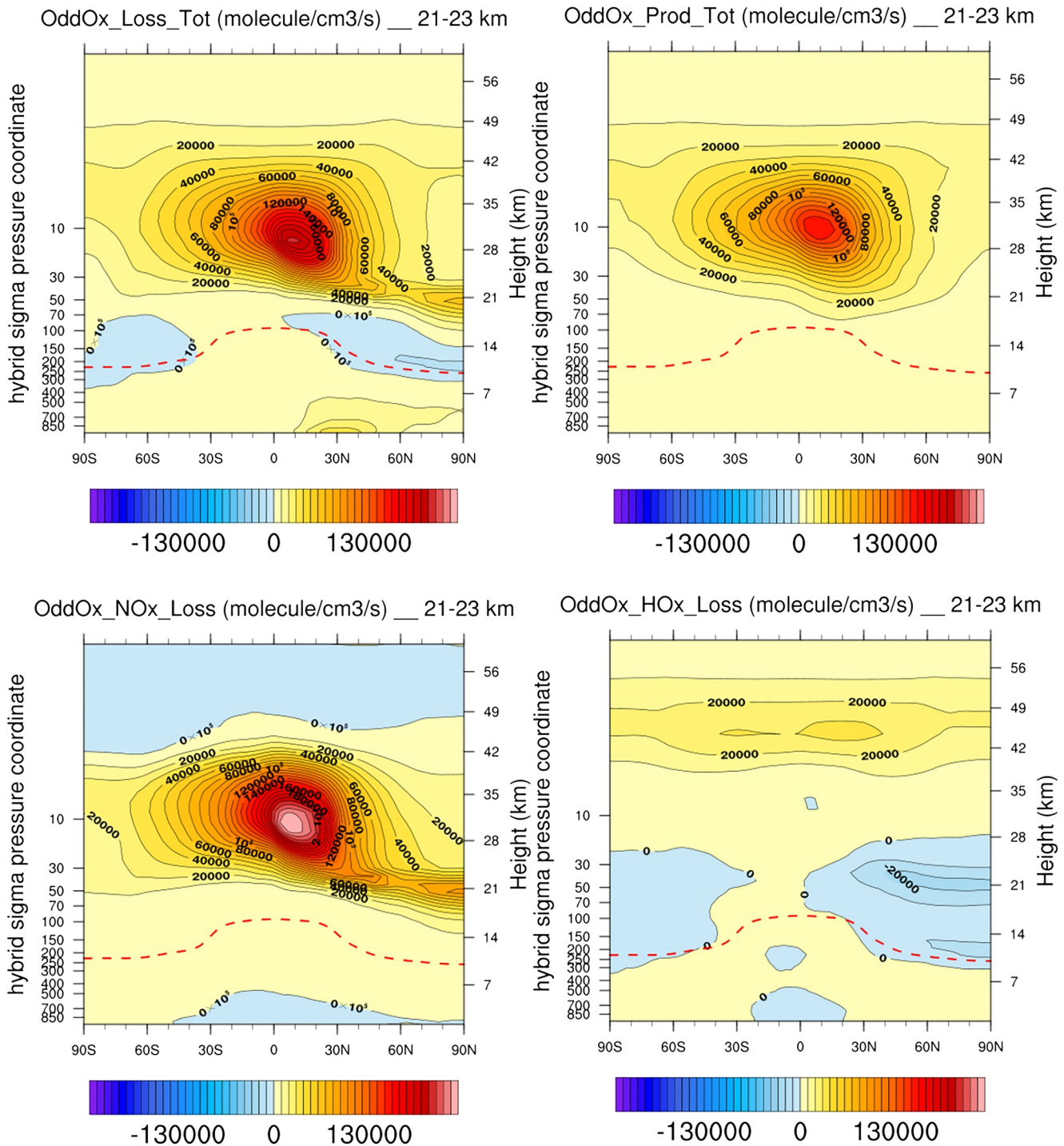
NO<sub>x</sub> perturbation from supersonic aircraft can either increase or decrease ozone depending on the relative balance of other chemicals in the ambient environment, such as NO<sub>x</sub>, HO<sub>x</sub>, and halogen radicals in the background atmosphere. In the lower stratosphere, the additional NO<sub>x</sub> from supersonic aircraft emissions would produce ozone, by smog chemistry as well as interfering with and decreasing the ozone loss from ClO<sub>x</sub>/BrO<sub>x</sub>-Ox and HO<sub>x</sub>-Ox catalytic cycles (Figures 6e and 6f). At higher altitudes, in the middle and upper stratosphere, the enhanced NO<sub>x</sub> and HO<sub>x</sub> induced from supersonic aircraft emissions are both acting as ozone-depleting substances and reduce the stratospheric and mesospheric ozone catalytically.

Figure 7 shows the Ox loss family cycles similar to that illustrated in Figure 6 but focusing on their variations in latitude and altitude. Using cruise altitude at 21–23 km as an example, Figure 7a shows the total Ox loss induced from supersonic aircraft emissions, with the positive values indicating the increased loss rate. The change in total Ox production rate is shown in Figure 7b. The maximums of total loss and production are both mainly concentrated over 10°S to 30°N ranging from 25 to 35 km. There is also a local peak of Ox loss over the NH polar region at the cruise altitude. As a result, the net Ox loss is mainly over the NH high latitudes owing to the offsetting effects between the total Ox loss and total Ox production, which is consistent with the ozone change shown in Figure 4a.

The distribution of the total Ox loss is mainly attributed to the NO<sub>x</sub>-Ox loss cycle among all four family cycles (Figures 7a and 7c), especially the Ox loss peak at the NH polar region. The contribution of the HO<sub>x</sub>-Ox loss cycle is primarily effective at higher altitudes, around 40–50 km, while losses from the other two cycles (Ox-Ox loss and ClO<sub>x</sub>/BrO<sub>x</sub>-Ox loss) are minimal.

Total column ozone is the total amount of atmospheric ozone in a given column, and it is important in determining the overall exposure to ultraviolet radiation at the Earth's surface. At a given location, the total column ozone change depends on both the transport and chemical processes—the ozone production in the upper troposphere and lower stratosphere, and the ozone reduction in the middle and upper stratosphere. Figure 8 shows the percent change in the annually averaged distribution of total column ozone for the sensitivity emission scenarios. For cruise altitudes ranging from 13 to 23 km, the emitted materials from the assumed fleet of supersonic aircraft can deplete as much as –5.6% (–20.42 DU) of total column ozone regionally at the NH high latitudes for the cruise altitudes at 21–23 km (Figure 8a).

The strong effect of total ozone change at the North Pole is mainly attributed to the NO<sub>x</sub>-Ox loss, as shown in Figure 7. For emissions occurring at altitudes between 13 and 17 km, the total column ozone change mostly shows an increase throughout the globe. Only a small ozone depletion is found over South Asia in the 15–17 km case (Figure S2c). This is due to the NO<sub>x</sub> emissions at these cruise altitudes largely increasing the ozone in the lower stratosphere. For emissions at higher altitudes (18+ km), the total column ozone depletion occurs throughout the globe, with a positive gradient from the tropics to the northern polar regions.



**Figure 7.** (a) Zonal annual average distribution of odd oxygen (Ox) total chemical loss rates calculated by summing up four families defined in Text S1; (b) total chemical production rates (defined in Text S1); (c) NO<sub>x</sub>-Ox loss; (d) HO<sub>x</sub>-Ox loss; (e) ClO<sub>x</sub>/BrO<sub>x</sub>-Ox loss, (f) O<sub>x</sub>-Ox loss. The above figures are shown for the cruise altitude at 21–23 km.

Quantitative estimates of the total column ozone changes for different latitude bands for both hemispheres and for the globally averaged values are detailed in Table S3. Cruise emissions at 13–15, 14–16, and 15–17 km increase the global average total column ozone by 0.27% (0.79 DU), 0.32% (0.94 DU), and 0.25% (0.76 DU), respectively. Emissions at altitudes of 16–18 km result in an extremely small net global total column ozone change of 0.005 DU (0.003%) where the NO<sub>x</sub>-induced ozone production can balance out the

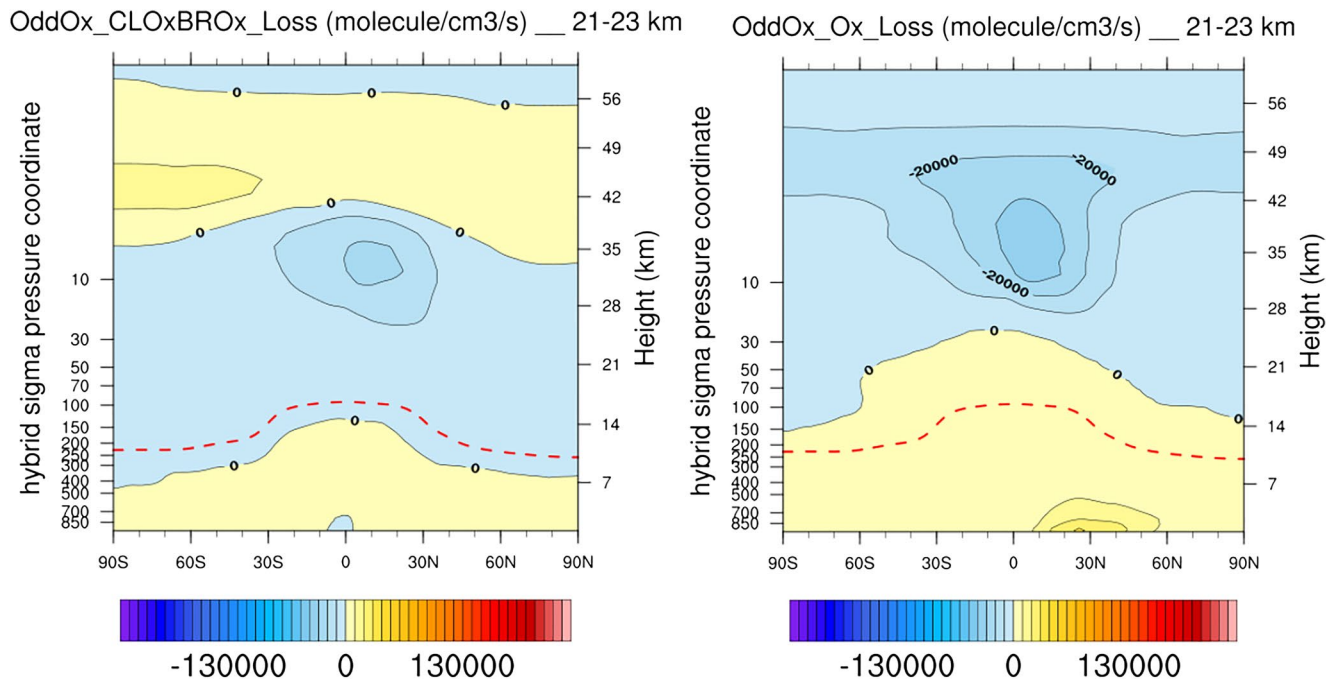


Figure 7. Continued.

ozone depletion. At cruise altitudes higher than 17 km, the supersonic emissions begin to cause a net negative globally averaged total column ozone change, and the ozone depletion increases with cruise height. The global total column ozone changes for cruise emissions at 17–19, 18–20, 19–21, and 21–23 km are calculated as  $-0.44\%$  ( $-1.28$  DU),  $-1.02\%$  ( $-3.03$  DU),  $-1.67\%$  ( $-4.98$  DU), and  $-2.72\%$  ( $-8.14$  DU), respectively. The inflection point, where the global total column ozone change switches from positive to negative, is near 17 km in our study, which is higher than the estimation of 14.5 km reported from earlier supersonic transport studies (e.g., Wuebbles, Dutta, Jain & Baughcum, 2003; Wuebbles, Dutta, Patten & Baughcum, 2003; Dutta et al., 2004). This difference can be attributed to several different factors, including the updated chemical reaction rates in WACCM, and the finer horizontal and vertical resolution now compared to the earlier models (used in Wuebbles, Dutta, Jain & Baughcum, 2003; Wuebbles, Dutta, Patten & Baughcum, 2003 and Dutta et al., 2004), which has improved the representation of chemical and physical processes. The difference in emission scenarios and background atmosphere can also contribute to this difference, for example, the previous study assumes a background atmosphere in 2020 while this study uses a 2050 atmosphere. The aircraft type is also different; the previous study from Dutta et al. (2004) assumes small supersonic business jets which can accommodate about 12–13 passengers, while this parametric study was based on a scenario derived for a much larger commercial supersonic aircraft with the capacity of 300 passengers.

The seasonal dependence of the total column ozone change in percent is shown in Figure 9. Total column ozone perturbation shows strong latitudinal and seasonal variations in each case. For a range of cruise altitudes between 13 and 23 km, the model derives a maximum NH column ozone depletion of about  $-6.8\%$  peaked in October over the northern polar region for the 21–23 km emission scenario. This number is about 45% of the stratospheric ozone depletion in the NH during 1990s. The seasonal dependence results from the combined effects of ozone production and loss varying with different seasons. In summer, the ozone production maximizes proportional to the amount of sunlight (Figure S4). Summertime NO<sub>x</sub>-induced ozone loss is also the largest, especially in the polar region (Pierce et al., 1999). For the 21–23 km case, the maximum ozone production and loss offset each other in June with a  $-3.8\%$  ozone change in the NH, which is less than  $-4.4\%$  in mid-October (Figure 9b).

Again, for emissions occurring at altitudes from 13 to 17 km, the total column ozone mainly shows an increase at all latitudes throughout the whole year. Only a small ozone depletion is found over 0–30°N in summer for the 15–17 km case (Figure S3c), which corresponds to the region over South Asia shown in



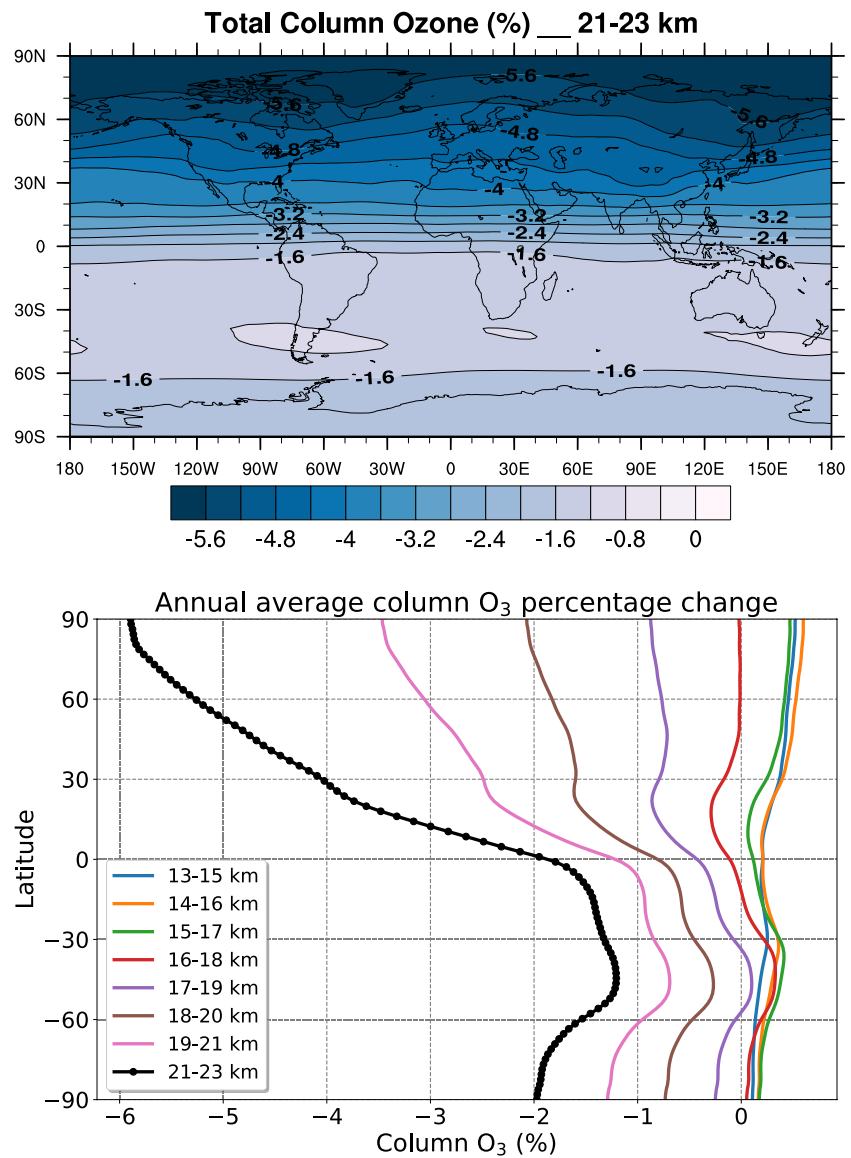


**Figure 8.** Calculated supersonic aircraft emission induced annually averaged changes in total column ozone (%) for cruise altitude at (a) 21–23 km and (b) its comparison with other cruise altitudes.

Figure S2c. The maximum column ozone augments peaks at the North Pole during the summer season (Figure S3). For emissions at higher altitudes (17–19 km and above), the ozone depletion occurs in the NH for all seasons, with the maximum ozone reduction occurring at high latitudes in the NH during the fall season in each emission scenario.

Figure 10 shows the sensitivity of the total column ozone change per unit of fuel consumption in the NH as a function of cruise altitude. The model predicts a strong dependence of ozone impact on cruise altitude. Below 17 km, the total column ozone impact for flying supersonic aircraft is calculated to be positive, but overall it is also very small. The ozone depletion increased sharply as the flight altitudes exceeded 17 km and effects get more and more negative for higher cruise altitudes. As the future supersonic aircraft designs are still under consideration, the actual emissions will depend on specific designs. The resulting impact scaled by fleet fuel consumption shown in Figure 10 can provide insights on the potential impacts on O<sub>3</sub> relative to a range of possible cruise altitudes, assuming an EI(NO<sub>x</sub>) = 20 combustor.

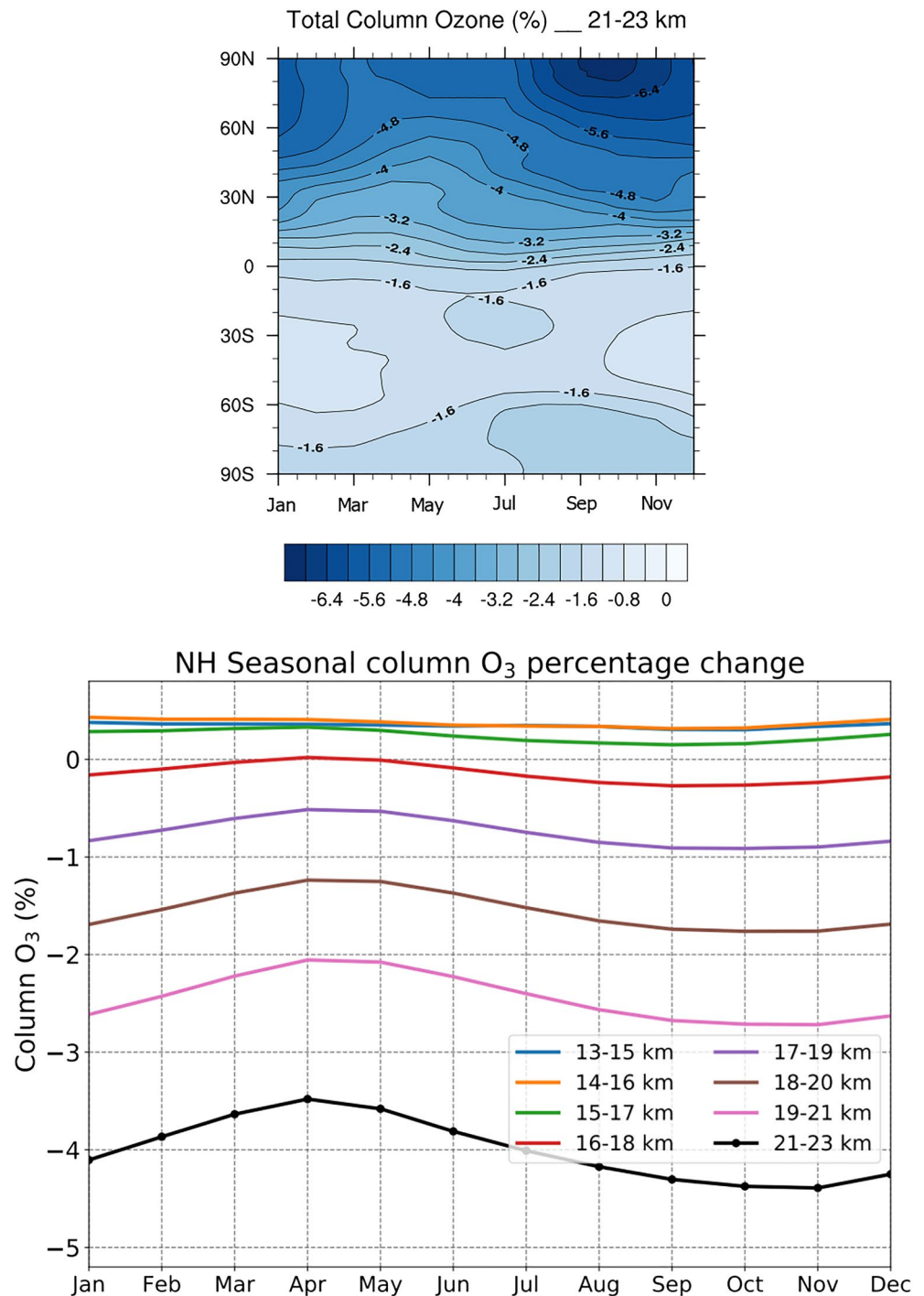


**Figure 9.** Seasonal dependence of calculated change in the total column ozone (%) for cruise altitude at (a) 21–23 km and (b) its comparison with other cruise altitudes in the NH.

#### 4.3. Radiative Forcing Response of Nitrogen Oxides and Water Vapor Emission

The radiative forcing from fleets of supersonic aircraft flying at a range of cruise altitudes are also examined. We use the PORT model to calculate the stratospheric-adjusted radiative forcing with the WACCM derived changes in ozone and water vapor for the set of sensitivity scenarios. The impact of supersonic transport on climate is associated with its emissions of CO<sub>2</sub>, H<sub>2</sub>O, NO<sub>x</sub>, SO<sub>2</sub>, and soot. In this study, the aircraft fleet

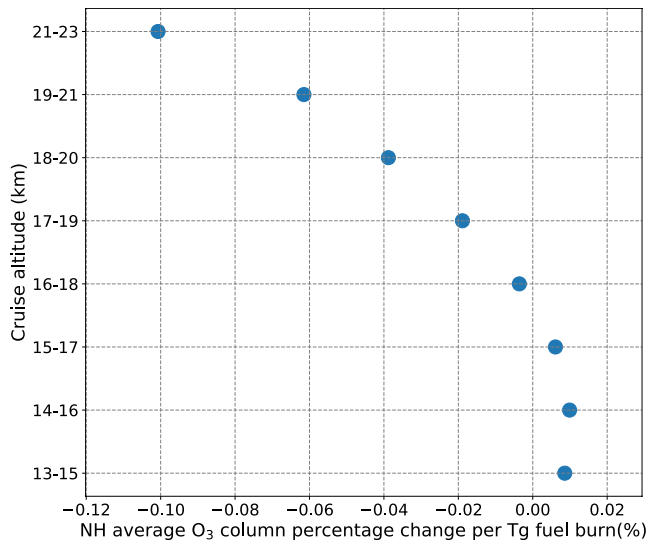


**Figure 10.** Northern Hemisphere total column ozone change (%) per Tg of fuel burn as a function of cruise altitudes from 13 to 23 km (e.g., 13–15 km means from 13 to 15 km with 2 km vertical cruise range). The total fuel burn is 47.18 Tg/yr in this study.

assumes no soot emissions and no sulfur in the fuel. For CO<sub>2</sub> emission, the fuel consumption of 47.18 Tg of jet fuel per year would increase atmospheric CO<sub>2</sub> by 0.019 ppmv/year, resulting in a positive (warming) radiative forcing of 4.1 mW/m<sup>2</sup>—too small to have a meaningful impact on stratospheric temperatures. This study only focuses on evaluating the potential radiative forcing impact of supersonic aircraft H<sub>2</sub>O and NO<sub>x</sub> emissions which are affecting the climate both directly and indirectly. The radiative forcing from the direct increase in stratospheric H<sub>2</sub>O, where natural levels of H<sub>2</sub>O are much smaller and its residence time is much longer than in the troposphere, can potentially induce significant radiative effect on climate. Previous studies have indicated that aircraft emissions of H<sub>2</sub>O in the troposphere are unlikely to be important contributors to climate change since the small perturbation in tropospheric H<sub>2</sub>O gets removed quickly by precipitation (Brasseur et al., 2016; Lee et al., 2010). In addition, the radiative forcing also results from indirect effects on atmospheric ozone as a result of H<sub>2</sub>O and NO<sub>x</sub> emissions. This can induce either a warming or cooling effect depending on the net ozone change at different cruise altitudes.

Figure 11 shows the calculated annual average change in stratospheric-adjusted forcing sensitivity due to the H<sub>2</sub>O and O<sub>3</sub> perturbations as a function of cruise altitude. The forcing sensitivity is calculated separately for the H<sub>2</sub>O and O<sub>3</sub> perturbations per unit of fuel burn. The derived radiative forcing changes before being scaled by fuel burn are listed in Table S4. The results indicate a monotonic increasing trend of H<sub>2</sub>O-induced forcing with increasing cruise altitude, which is consistent with the enhanced H<sub>2</sub>O perturbation. With H<sub>2</sub>O emission at higher altitudes, the derived forcing sensitivity increases, which indicates a strong warming impact on the surface. The forcing sensitivity calculated here can be used to estimate the warming effect induced by perturbing stratospheric H<sub>2</sub>O at the corresponding emission altitudes. The maximum forcing of H<sub>2</sub>O changes is calculated from the 21–23 km case, with a sensitivity of 1.12 mW m<sup>-2</sup> Tg<sup>-1</sup> fuel/yr and radiative forcing of 53.10 mW m<sup>-2</sup> for a supersonic fleet fuel use of 47.18 Tg/yr of jet fuel at cruise. This number is comparable to the radiative

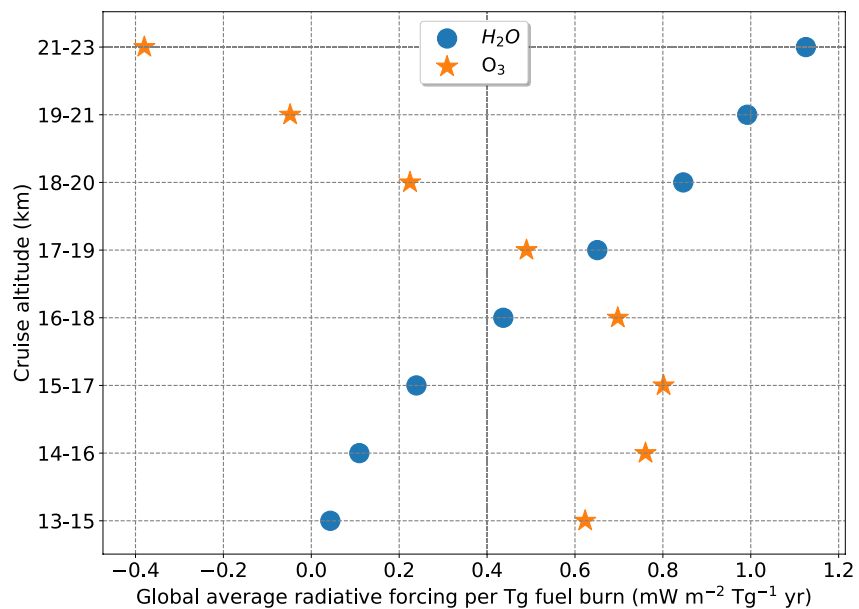


**Figure 11.** Annual and global average change in the stratospheric-adjusted radiative forcing per Tg of fuel burn (mW m<sup>-2</sup> Tg<sup>-1</sup> yr) as a function of cruise altitudes for the changes in H<sub>2</sub>O and O<sub>3</sub>. The total cruise fuel burn is 47.18 Tg/yr in this study.

forcing of  $57.4 \text{ mW m}^{-2}$  induced by contrail cirrus from all the subsonic aircraft operated in 2018 (Lee et al., 2020).

Forcing changes calculated for the perturbed ozone are more complicated than  $\text{H}_2\text{O}$ . Starting from a cruise altitude of 13–15 km, the forcing trend of ozone perturbation indicates an increase with altitude followed by a decrease with cruise altitude. As a greenhouse gas, ozone increases in the troposphere, due to the  $\text{NO}_x$  emission, greatly enhances the downward terrestrial longwave radiation to the ground, which induces a warming effect at the surface. In contrast, the ozone depletion in the stratosphere results in a cooling effect. Thus, the overall radiative forcing effect from ozone perturbation in each scenario is determined by the two competing processes. The model results illustrate that the cooling from the stratospheric ozone depletion becomes dominant over the warming induced from the tropospheric ozone increase at cruise altitudes of 19+ km, causing a net cooling effect from the ozone perturbation.

## 5. Discussion and Conclusions

This study has evaluated the sensitivity of the potential environmental effects at different cruise altitudes of supersonic transport on atmospheric ozone and radiative forcing. A series of sensitivity studies of possible future cruise altitudes were conducted to evaluate the relative atmospheric response from  $\text{NO}_x$  and  $\text{H}_2\text{O}$  emissions for a fleet of supersonic aircraft assumed to be operating in 2050. A fixed fleet fuel use and geographical distribution is assumed in this sensitivity study.

For a range of cruise altitudes from 13 to 23 km evaluated in this study, the resulting ozone impacts depending on the altitude and can be either positive or negative when examining the annual and global averaging total ozone column change. For emissions in the upper troposphere and lower stratosphere, such as the cases for cruise altitude between 13 and 17 km, the total column ozone indicates a slight increase. This increase is due to the combined effects from a reduction in the ozone loss rates due to interference reactions and the direct effects of enhanced ozone production from  $\text{NO}_x$  emissions, as well as the ozone self-healing effect. At these altitudes, the ozone chemistry is affected by the coupling of  $\text{HO}_x/\text{NO}_x/\text{ClO}_x/\text{BrO}_x$  chemistry and the resulting ozone impact is less significant and much less dependent on the altitude of the aircraft emissions. At higher cruise altitudes from 17 to 23 km, stratospheric ozone is reduced, primarily as a result of the  $\text{NO}_x$ - $\text{O}_3$  catalytic cycles, and the magnitude of the ozone destruction increases with the higher cruise altitude. The resulting changes in total column ozone at these altitudes are highly dependent on the cruise altitude. A cruise altitude from 16 to 18 km shows a minimal total column ozone change resulting from the offsetting effects of ozone production and reduction at different heights. The inflection point is around 17 km in terms of total column ozone change, where the effect from supersonic emission on ozone transitions from the column ozone increase to the column ozone decrease. The maximum total column ozone loss occurs in the NH high latitudes in the fall season. With higher cruise altitudes, more ozone depletion is found in the SH as more emitted  $\text{NO}_x$  and  $\text{H}_2\text{O}$  are lifted upward and transported southward across the equator.

Some assumptions in this study also contribute to uncertainties in the result effects on ozone and climate. For example, the background atmosphere is assumed to be under volcanic clean conditions in the 2050 time period. The ozone depletion could be more significantly affected if emissions were occurring in a background of a major volcanic eruption and its influence on heterogeneous chemistry; these effects would typically last for up to 3 years. Plume chemistry is not considered in this study. Plume processes can be important in the initial plume if comparing with the well-mixed case at short time intervals, but prior study (Vohralik et al., 2008) suggests it is much less important on comparing the results after a number of days. Effects from emissions of particles and particle precursors, including any sulfur in the fuel, need to also be considered in future studies. We anticipate the effects from contrails would be negligible since the stratospheric water vapor concentrations are very low (4–5 ppmv) and thus contrails in the stratosphere would not be expected to grow or persist for very long.

The viability of building fleets of supersonic aircraft will also be affected by climate policy decisions and perhaps by the availability of sustainable aviation fuels. More sensitivity studies are needed to explore the possible ozone perturbation effects under different atmospheric conditions and to consider how low- $\text{NO}_x$  combustion technology would affect the result, allowing a separation of the  $\text{NO}_x$  and  $\text{H}_2\text{O}$  emission effects on stratospheric ozone. The feedback effects resulting from chemical-dynamical interactions are also not

taken into account in the specified dynamics simulations, which could also have a likely small effect on the resulting ozone changes.

This study looked at a range of cruise altitudes that encompass the range the concepts that have been discussed by the industry for commercial supersonic aircraft. The sensitivity study is based on an assumed Mach 2.4 300-passenger conceptual supersonic airliner and a projected network based on its 5,000 nautical mile range that was developed in the 1990s (Kawa et al., 1999). As a consequence, the fleet fuel use in these studies is likely larger than any of the much smaller business jets being considered. Likewise, the range, projected markets, utilization, and fleet sizes for actual supersonic transport under consideration could be much different, resulting in differences in the geographical patterns of the emissions as well as the levels of emissions. If developers are successful at developing designs with low sonic boom, then the geographical distributions could also be quite different because of flights occurring over land. When viewed as impact scaled by fleet fuel use, this study provides insights on the potential impacts on ozone relative to cruise altitudes. As such, this study indicates that consideration of low NO<sub>x</sub> combustors could be important if large fleets of supersonic aircraft flying at the highest altitudes were to become viable. In future studies, the environmental effects of more specific concepts or markets would be useful to the aeronautical industry since business jets and commercial airliners can differ greatly in their markets and constraints.

### Data Availability Statement

The atmospheric modeling data sets used in the development of the tables and figures from this study are available to the community through the Illinois Data Bank (IDB), a public access repository at the University of Illinois at Urbana-Champaign (UIUC). The website for our data set at the University of Illinois Data Bank is: <https://databank.illinois.edu/datasets/IDB-9081595>.

### Acknowledgments

The authors thank Simone Tilmes for helping with SST/ICE data files to drive the WACCM simulations, and Jean-Francois Lamarque and Francis Vitt for providing suggestions on running PORT. The authors would like to acknowledge high-performance computing support from Cheyenne (doi:10.5065/D6RX99HX) provided by the NCAR's Computational and Information Systems Laboratory, sponsored by the National Science Foundation. The authors from the University of Illinois were supported in part by the Boeing Company and by the U.S. Federal Aviation Administration (13-C-AJFE-UI-029).

### References

- Baughcum, S. L., & Henderson, S. C. (1995). *Aircraft emission inventories projected in year 2015 for a High Speed Civil transport (HSCT) universal airline network* (NASA CR-4659).
- Baughcum, S. L., & Henderson, S. C. (1998). *Aircraft emission scenarios projected in Year 2015 for the NASA Technology Concept Aircraft (TCA) high speed civil transport* (NASA CR-1998-207635).
- Baughcum, S. L., Henderson, S. C., Hertel, P. S., Maggiora, D. R., & Oncina, C. A. (1994). *Stratospheric emissions effects database development*. (NASA CR-4592) Any of the NASA reports cited in this study can be downloaded from the NASA Technical Reports server at <https://ntrs.nasa.gov/>
- Baughcum, S. L., Plumb, I. C., & Vohralik, P. F. (2003). Stratospheric ozone sensitivity to aircraft cruise altitudes and NO<sub>x</sub> emissions. In *European Conference on Aviation, Atmosphere and Climate (AAC)*. (Vol. 83, pp. 145–150). Friedrichshafen, Germany.
- Brasseur, G. P. (2020). *The ozone layer: From discovery to recovery*. American Meteorological Society.
- Brasseur, G. P., Gupta, M., Anderson, B. E., Balasubramanian, S., Barrett, S., Duda, D., et al. (2016). Impact of aviation on climate: FAA's aviation climate change research initiative (ACCRI) phase II. *Bulletin of the American Meteorological Society*, 97(4), 561–583. <https://doi.org/10.1175/BAMS-D-13-00089.1>
- Brasseur, G. P., & Solomon, S. (2005). *Aeronomy of the Middle Atmosphere* (Vol. 3217, p. 3300). Dordrecht, The Netherlands: Springer.
- Bretherton, C. S., & Park, S. (2009). A new moist turbulence parameterization in the Community Atmosphere Model. *Journal of Climate*, 22(12), 3422–3448. <https://doi.org/10.1175/2008JCLI2556.1>
- Butchart, N. (2014). The Brewer-Dobson circulation. *Reviews of Geophysics*, 52(2), 157–184. <https://doi.org/10.1002/2013RG000448>
- Butler, A. H., Daniel, J. S., Portmann, R. W., Ravishankara, A. R., Young, P. J., Fahey, D. W., & Rosenlof, K. H. (2016). Diverse policy implications for future ozone and surface UV in a changing climate. *Environmental Research Letters*, 11(6), 064017. <https://doi.org/10.1088/1748-9326/11/6/064017>
- Conley, A. J., Lamarque, J. F., Vitt, F., Collins, W. D., & Kiehl, J. (2013). PORT, a CESM tool for the diagnosis of radiative forcing. *Geoscientific Model Development*, 6(2), 469–476. <https://doi.org/10.5194/gmd-6-469-2013>
- Crutzen, P. (1974). Estimates of possible variations in total ozone due to natural causes and human activities. *Ambio*, 3, 201–210.
- Crutzen, P., & Ehhalt, D. (1977). Effects of nitrogen fertilizers and combustion on the stratospheric ozone layer. *Ambio*, 6, 112–117.
- Crutzen, P. J. (1972). SST's: A threat to the Earth's ozone shield. *Ambio*, 1, 41–51.
- Dameris, M., Grewe, V., Köhler, I., Sausen, R., Brühl, C., Groöf, J. U., & Steil, B. (1998). Impact of aircraft NO<sub>x</sub> emissions on tropospheric and stratospheric ozone. Part II: 3-D model results. *Atmospheric Environment*, 32(18), 3185–3199. [https://doi.org/10.1016/S1352-2310\(97\)00505-0](https://doi.org/10.1016/S1352-2310(97)00505-0)
- Dutta, M., Patten, K., & Wuebbles, D. (2004). *Parametric analyses of potential effects on stratospheric and tropospheric ozone chemistry by a fleet of supersonic business jets projected in a 2020 atmosphere* (National Aeronautics and Space Administration report NASA/CR—2004-213306).
- Fels, S. B., Mahlman, J. D., Schwarzkopf, M. D., & Sinclair, R. W. (1980). Stratospheric sensitivity to perturbations in ozone and carbon dioxide: Radiative and dynamical response. *Journal of the Atmospheric Sciences*, 37(10), 2265–2297. [https://doi.org/10.1175/1520-0469\(1980\)037<2265:sstpio>2.0.co;2](https://doi.org/10.1175/1520-0469(1980)037<2265:sstpio>2.0.co;2)
- Froidevaux, L., Kinnison, D. E., Wang, R., Anderson, J., & Fuller, R. A. (2019). Evaluation of CESM1 (WACCM) free-running and specified dynamics atmospheric composition simulations using global multispecies satellite data records. *Atmospheric Chemistry and Physics*, 19(7), 4783–4821. <https://doi.org/10.5194/acp-19-4783-2019>

- García, R. R., Smith, A. K., Kinnison, D. E., Cámara, Á. D. L., & Murphy, D. J. (2017). Modification of the gravity wave parameterization in the Whole Atmosphere Community Climate Model: Motivation and results. *Journal of the Atmospheric Sciences*, *74*(1), 275–291. <https://doi.org/10.1175/JAS-D-16-0104.1>
- García, R. R., Yue, J., & Russell, J. M., III (2019). Middle atmosphere temperature trends in the twentieth and twenty-first centuries simulated with the Whole Atmosphere Community Climate Model (WACCM). *Journal of Geophysical Research: Space Physics*, *124*(10), 7984–7993. <https://doi.org/10.1029/2019JA026909>
- Gent, P. R., Danabasoglu, G., Donner, L. J., Holland, M. M., Hunke, E. C., Jayne, S. R., et al. (2011). The community climate system model version 4. *Journal of Climate*, *24*(19), 4973–4991. <https://doi.org/10.1175/2011JCLI4083.1>
- Grewe, V., Plohr, M., Cerino, G., Di Muzio, M., Deremaux, Y., Galerneau, M., et al. (2010). Estimates of the climate impact of future small-scale supersonic transport aircraft—results from the HISAC EU-project. *The Aeronautical Journal*, *114*(1153), 199–206. <https://doi.org/10.1017/s00019240000364x>
- Grewe, V., Stenke, A., Ponater, M., Sausen, R., Pitari, G., Iachetti, D., et al. (2007). Climate impact of supersonic air traffic: An approach to optimize a potential future supersonic fleet—results from the EU-project SCENIC. *Atmospheric Chemistry and Physics*, *7*(19), 5129–5145. <https://doi.org/10.5194/acp-7-5129-2007>
- Grooß, J.-U., Bruhl, C., & Peter, T. (1998). Impact of aircraft emissions on tropospheric and stratospheric ozone, I: Chemistry and 2-D model results. *Atmospheric Environment*, *32*, 3173–3184. [https://doi.org/10.1016/S1352-2310\(98\)00016-8](https://doi.org/10.1016/S1352-2310(98)00016-8)
- Haenel, F. J., Stiller, G. P., Von Clarmann, T., Funke, B., Eckert, E., Glatthor, N., et al. (2015). Reassessment of MIPAS age of air trends and variability. *Atmospheric Chemistry and Physics*, *15*(22), 13161–13176. <https://doi.org/10.5194/acp-15-13161-2015>
- Hall, T. M., & Plumb, R. A. (1994). Age as a diagnostic of stratospheric transport. *Journal of Geophysical Research*, *99*(D1), 1059–1070. <https://doi.org/10.1029/93JD03192>
- Johnston, H. (1971). Reduction of stratospheric ozone by nitrogen oxide catalysts from supersonic transport exhaust. *Science*, *173*(3996), 517–522. <https://doi.org/10.1126/science.173.3996.517>
- Johnston, H. S., Kinnison, D. E., & Wuebbles, D. J. (1989). Nitrogen oxides from high-altitude aircraft: An update of potential effects on ozone. *Journal of Geophysical Research*, *94*(D13), 16351–16363. <https://doi.org/10.1029/JD094iD13p16351>
- Kawa, S. R., Anderson, J. G., Baughcum, S. L., Brock, C. A., Brune, W. H., Cohen, R. C., et al. (1999). *Assessment of the effects of high-speed aircraft in the stratosphere: 1998* (National Aeronautics and Space Administration Report NASA/TMM 1999-209237).
- Kinnison, D., Brasseur, G., Baughcum, S. L., Zhang, J., & Wuebbles, D. (2020). The impact on the ozone layer of a potential fleet of civil hypersonic aircraft. *Earth's Future*, *8*, e2020EF001626. <https://doi.org/10.1029/2020EF001626R10.1029/2020EF001626>
- Kinnison, D. E., Brasseur, G. P., Walters, S., García, R. R., Marsh, D. R., Sassi, F., et al. (2007). Sensitivity of chemical tracers to meteorological parameters in the MOZART-3 chemical transport model. *Journal of Geophysical Research*, *112*(D20), D20302. <https://doi.org/10.1029/2006JD007879>
- Kunz, A., Pan, L. L., Konopka, P., Kinnison, D. E., & Tilmes, S. (2011). Chemical and dynamical discontinuity at the extratropical tropopause based on START08 and WACCM analyses. *Journal of Geophysical Research*, *116*(D24), D24302. <https://doi.org/10.1029/2011JD016686>
- Lamarque, J. F., Emmons, L. K., Hess, P. G., Kinnison, D. E., Tilmes, S., Vitt, F., et al. (2012). CAM-chem: Description and evaluation of interactive atmospheric chemistry in the Community Earth System Model. *Geoscientific Model Development*, *5*(2), 369–411. <https://doi.org/10.5194/gmd-5-369-2012>
- Lee, D. S., Fahey, D. W., Skowron, A., Allen, M. R., Burkhardt, U., Chen, Q., et al. (2020). The contribution of global aviation to anthropogenic climate forcing for 2000 to 2018. *Atmospheric Environment*, *244*, 117834. <https://doi.org/10.1016/j.atmosenv.2020.117834>
- Lee, D. S., Pitari, G., Grewe, V., Gierens, K., Penner, J. E., Petzold, A., et al. (2010). Transport impacts on atmosphere and climate: Aviation. *Atmospheric Environment*, *44*(37), 4678–4734. <https://doi.org/10.1016/j.atmosenv.2009.06.005>
- Lin, S. J. (2004). A “vertically Lagrangian” finite-volume dynamical core for global models. *Monthly Weather Review*, *132*(10), 2293–2307. [https://doi.org/10.1175/1520-0493\(2004\)132<2293:avfcd>2.0.co;2](https://doi.org/10.1175/1520-0493(2004)132<2293:avfcd>2.0.co;2)
- Marsh, D. R., Mills, M. J., Kinnison, D. E., Lamarque, J. F., Calvo, N., & Polvani, L. M. (2013). Climate change from 1850 to 2005 simulated in CESM1 (WACCM). *Journal of Climate*, *26*(19), 7372–7391. <https://doi.org/10.1175/JCLI-D-12-00558.1>
- Matthes, K., Marsh, D. R., García, R. R., Kinnison, D. E., Sassi, F., & Walters, S. (2010). Role of the QBO in modulating the influence of the 11 year solar cycle on the atmosphere using constant forcings. *Journal of Geophysical Research*, *115*(D18), D18110. <https://doi.org/10.1029/2009JD013020>
- Meinshausen, M., Smith, S. J., Calvin, K., Daniel, J. S., Kainuma, M. L. T., Lamarque, J. F., et al. (2011). The RCP greenhouse gas concentrations and their extensions from 1765 to 2300. *Climatic Change*, *109*(1–2), 213–241. <https://doi.org/10.1007/s10584-011-0156-z>
- Morgenstern, O., Hegglin, M. I., Rozanov, E., O'Connor, F. M., Abraham, N. L., Akiyoshi, H., et al. (2017). Review of the global models used within phase 1 of the Chemistry-Climate Model Initiative (CCMI). *Geoscientific Model Development*, *10*, 639–671. <https://doi.org/10.5194/gmd-10-639-2017>
- Neale, R. B., Richter, J., Park, S., Lauritzen, P. H., Vavrus, S. J., Rasch, P. J., & Zhang, M. (2013). The mean climate of the Community Atmosphere Model (CAM4) in forced SST and fully coupled experiments. *Journal of Climate*, *26*(14), 5150–5168. <https://doi.org/10.1175/JCLI-D-12-00236.1>
- Neu, J. L., Flury, T., Manney, G. L., Santee, M. L., Livesey, N. J., & Worden, J. (2014). Tropospheric ozone variations governed by changes in stratospheric circulation. *Nature Geoscience*, *7*(5), 340–344. <https://doi.org/10.1038/NGEO2138>
- Penner, J. E., Lister, D. H., Griggs, D. J., Dokken, D. J., & McFarland, M. (Eds.). (1999). *Aviation and the global atmosphere* (pp. 1–373). Cambridge, UK: Cambridge University Press.
- Pierce, R. B., Al-Saadi, J. A., Fairlie, T. D., Olson, J. R., Eckman, R. S., Grose, W. L., et al. (1999). Large-scale stratospheric ozone photochemistry and transport during the POLARIS campaign. *Journal of Geophysical Research*, *104*(D21), 26525–26545. <https://doi.org/10.1029/1999JD900395>
- Pitari, G., & Mancini, E. (2001). Climatic impact of future supersonic aircraft: Role of water vapour and ozone feedback on circulation. *Physics and Chemistry of the Earth, Part C: Solar, Terrestrial & Planetary Science*, *26*(8), 571–576. [https://doi.org/10.1016/S1464-1917\(01\)00049-6](https://doi.org/10.1016/S1464-1917(01)00049-6)
- Pitari, G., Mancini, E., Rogers, H. L., Dessens, O., Isaksen, I. S. A., & Rognerud, B. (2004). A 3-D model intercomparison of the effects of future supersonic aircraft on the chemical composition of the stratosphere. In *Proceedings of the 2003 AAC-Conference*. (pp. 166–172). Friedrichshafen, Germany.
- Portmann, R. W., Daniel, J. S., & Ravishankara, A. R. (2012). Stratospheric ozone depletion due to nitrous oxide: Influences of other gases. *Philosophical Transactions of the Royal Society B: Biological Sciences*, *367*(1593), 1256–1264. <https://doi.org/10.1098/rstb.2011.0377>
- Ravishankara, A. R., Daniel, J. S., & Portmann, R. W. (2009). Nitrous oxide (N<sub>2</sub>O): The dominant ozone-depleting substance emitted in the 21st century. *Science*, *326*(5949), 123–125. <https://doi.org/10.1126/science.1176985>

- Tilmes, S., Lamarque, J.-F., Emmons, L. K., Kinnison, D. E., Marsh, D., Garcia, R. R., et al. (2016). Representation of the community earth system model (CESM1) CAM4-chem within the Chemistry-Climate Model Initiative (CCMI). *Geoscientific Model Development*, 9(5), 1853–1890. <https://doi.org/10.5194/gmd-9-1853-2016>
- Van Vuuren, D. P., Edmonds, J., Kainuma, M., Riahi, K., Thomson, A., Hibbard, K., et al. (2011). The representative concentration pathways: An overview. *Climatic Change*, 109(1–2), 5–31. <https://doi.org/10.1007/s10584-011-0148-z>
- Vohralik, P. F., Randeniya, L. K., Plumb, I. C., & Baughcum, S. L. (2008). Effect of plume processes on aircraft impact. *Journal of Geophysical Research*, 113(D5), D05312. <https://doi.org/10.1029/2007JD008982>
- Waugh, D., & Hall, T. (2002). Age of stratospheric air: Theory, observations, and models. *Reviews of Geophysics*, 40(4), 1. <https://doi.org/10.1029/2000RG000101>
- World Meteorological Organization (WMO) (2018). *Scientific assessment of ozone depletion: 2018* (Global Ozone Research and Monitoring Project-Report No. 58). (p. 588). Geneva, Switzerland: World Meteorological Organization.
- Wuebbles, D. J., Dutta, M., Jain, A. K., & Baughcum, S. L. (2003). Radiative forcing on climate from stratospheric aircraft emissions. In *European Conference on Aviation, Atmosphere and Climate (AAC)* (Vol. 30, pp. 184–189). Friedrichshafen, Germany.
- Wuebbles, D. J., Dutta, M., Patten, K. O., & Baughcum, S. L. (2003). Parametric study of potential effects of aircraft emissions on stratospheric ozone. In *European Conference on Aviation, Atmosphere and Climate (AAC)* (Vol. 30, pp. 140–144). Friedrichshafen, Germany.
- Yang, B., Qian, Y., Lin, G., Leung, L. R., Rasch, P. J., Zhang, G. J., et al. (2013). Uncertainty quantification and parameter tuning in the CAM5 Zhang-McFarlane convection scheme and impact of improved convection on the global circulation and climate. *Journal of Geophysical Research: Atmospheres*, 118(2), 395–415. <https://doi.org/10.1029/2012JD018213>
- Zhang, G. J., & McFarlane, N. A. (1995). Sensitivity of climate simulations to the parameterization of cumulus convection in the Canadian Climate Centre general circulation model. *Atmosphere-Ocean*, 33(3), 407–446. <https://doi.org/10.1080/07055900.1995.9649539>
- Zhang, J., Wuebbles, D. J., Kinnison, D. E., & Baughcum, S. L. (2021). Potential impacts of supersonic aircraft emissions on ozone and resulting forcing on climate. *Journal of Geophysical Research: Atmospheres*, 126, e2020JD034130. <https://doi.org/10.1029/2020JD034130>